ALMA MATER STUDIORUM · UNIVERSITÀ DI BOLOGNA

Scuola di Scienze
Dipartimento di Fisica e Astronomia
Corso di Laurea in Fisica

Quantum Error Correction with the IBM quantum experience

Relatore:
Prof.ssa Elisa Ercolessi

Correlatore:
Dott. Davide Vodola

Presentata da:
Matteo Barbieri

Anno Accademico 2021/2022

Abstract

Mentre si svolgono operazioni su dei qubit, possono avvenire vari errori, modificando così l'informazione da essi contenuta. La *Quantum Error Correction* costruisce algoritmi che permettono di tollerare questi errori e proteggere l'informazione che si sta elaborando. Questa tesi si focalizza sui *codici a 3 qubit*, che possono correggere un errore di tipo *bit-flip* o un errore di tipo *phase-flip*. Più precisamente, all'interno di questi algoritmi, l'attenzione è posta sulla *procedura di encoding*, che punta a proteggere meglio dagli errori l'informazione contenuta da un qubit, e la *syndrome measurement*, che specifica su quale qubit è avvenuto un errore senza alterare lo stato del sistema. Inoltre, sfruttando la procedura della *syndrome measurement*, è stata stimata la probabilità di errore di tipo *bit-flip* e *phase-flip* su un qubit attraverso l'utilizzo della *IBM quantum experience*.

Abstract

While performing quantum computations several errors may occur on the qubits involved, thus modifying the information they store. *Quantum Error Correction* constructs algorithms to tolerate these errors and protect the information which is been processed. This dissertation focuses on *3-qubit codes* which can correct for *bit-flip* or *phase-flip* errors. More precisely, within these algorithms, the attention is driven on the *encoding procedure*, which aims to better protect from errors the information stored by a qubit, and on the *syndrome measurement*, which specifies on which qubit an error has occurred without altering the state of the system. Furthermore exploiting the *syndrome measurement* procedure the error probability of a *bit-flip* and a *phase-flip* error on a qubit has been assessed using the *IBM quantum experience.*

Contents

Introduction

Quantum Information Science is an interdisciplinary field that seeks to understand the analysis, processing, and transmission of information using Quantum Mechanics principles. This manner of handling information processing promises to overtake the classical computer's capabilities in some areas [1]. The devices that perform quantum computation are *quantum computers*, which operate using *qubits* as the basic unit of quantum information, that can be built using different physical systems such as neutral atoms [2], ion traps [3], superconductors [4], photons [5], or anyons (topological quantum computing) [6]. However there is an obstacle which needs to be solved common to all these devices: qubits suffer quantum decoherence, i.e. it is difficult to keep the qubit in a quantum superposition. Therefore quantum computers need *Quantum Error Correction (QEC)*, which is the theoretical topic that guides the experimental effort to build fault-tolerant quantum computers [7]. QEC gives the tools to increase the state fidelity and nowadays it has been proven to be realizable for example on superconducting circuits [8] and on trapped-ion quantum computers [9].

Avoiding the specifics of each quantum hardware, the goal of this thesis is to understand what a quantum error is and to analyze the *3-qubit Shor codes* for *bit-flip* and *phase-flip* errors, focusing primarily on the *encoding* procedure, which aims to better protect the information stored in a qubit, and the *error detection* procedure, that indicates the qubit on which an error has occurred and that is then exploited to evaluate the error probability on a qubit on a real quantum device.

More precisely this dissertation is structured in 3 chapters: Chapter 1 gives the fundamental concepts needed for the topic at hand, namely postulates of Quantum Mechanics for *pure states* and *mixed states*, and of course *qubits*, *quantum gates* and *quantum circuits*, which are necessary to implement quantum algorithms. Then Chapter 2 discusses the basis of QEC [10], explaining the differences with classical error correction, and illustrating what a *quantum error* is. Afterwards the focus is moved on the *3-qubit codes* which can correct for *bit-flip* or *phase-flip* errors. Common to both of them, the *encoding* procedure is deeply analyzed, justifying its purpose with both analytical computations and a computer simulation with the Python module *Qutip*. Furthermore the *error detection* procedure, involving *syndrome measurement*, is thoroughly discussed as it is fundamental in this chapter, but also in the following one. To conclude in

Chapter 2 the *9-qubit Shor code* [11] is introduced as an example of a QEC procedure that exploiting more qubits can correct for more than one error. Finally in Chapter 3 the method to perform *syndrome measurements*, introduced for the *3-qubit codes* in Chapter 2, is taken advantage of in order to evaluate the error probability on a single real qubit for both *bit-flip* and *phase-flip* errors. This is done by implementing quantum circuits via the Python module *Qiskit* and running them on the 5-qubit real quantum device *ibmq_manila* that IBM makes available on the cloud.

Chapter 1

Fundamentals of Quantum Mechanics for QEC

Quantum computation is done on quantum systems which are known as *qubits* [12], i.e. two-level systems. Therefore the first section of this chapter will introduce them in order to be able to make examples in which they are involved. In order to understand the subject one has to have some knowledge of Quantum Mechanics. Since the concept of *mixed states* is present in this dissertation the *density matrix* formalism [12] needs to be introduced and, for the sake of clarity, before doing this, the *vector state's* formalism will be revised, which will come in handy for *pure states* [12], that will be widely exploited throughout this thesis. The two formalisms are indeed discussed in Sec. 1.2. To conclude this chapter *quantum gates* and *quantum circuits* will be introduced in Sec. 1.3 [12].

1.1 Qubits

In classical computing the basic unit of information is the classical bit, which can take the value 0 or 1. In quantum computing the basic unit of quantum information is the quantum bit, known as *qubit* [12], which is a two-state quantum-mechanical system, mathematically described as object belonging to a two-dimensional Hilbert space.

While a classical bit is either in the state 0 or in the state 1, a qubit can be, as it is a quantum object, in a superposition of the two:

$$|\psi\rangle = \alpha\,|0\rangle + \beta\,|1\rangle\,, \tag{1.1}$$

when $\alpha, \beta \in \mathbb{C}$. The set $\{|0\rangle\,, |1\rangle\}$ is known as *computational basis* and form an orthonormal basis for the two-dimensional Hilbert vector space. In the more common column-vectors notation they are written as:

$$|0\rangle = \begin{pmatrix} 1 \\ 0 \end{pmatrix}, \quad |1\rangle = \begin{pmatrix} 0 \\ 1 \end{pmatrix}.$$

This implies that when one measures the state of a qubit the result can be either $|0\rangle$ with probability $|\alpha|^2$ or $|1\rangle$ with probability $|\beta|^2$. Obviously probabilities are normalized to one so that $|\alpha|^2 + |\beta|^2 = 1$.

A Hilbert space is a linear space, thus one can change the basis in which they represent the space's element. For example there are the basis $\{|+\rangle, |-\rangle\}$ and $\{|+\rangle_y, |-\rangle_y\}$. These basis can be written in the computational basis as:

$$|+\rangle = \frac{|0\rangle + |1\rangle}{\sqrt{2}} \quad |-\rangle = \frac{|0\rangle - |1\rangle}{\sqrt{2}}, \tag{1.2}$$

$$|+\rangle_y = \frac{|0\rangle + i\,|1\rangle}{\sqrt{2}} \quad |-\rangle_y = \frac{|0\rangle - i\,|1\rangle}{\sqrt{2}}. \tag{1.3}$$

These three basis that have been introduced are the eigenkets of the Pauli matrices (Eq. (1.29), (1.30), (1.31)): $\{|0\rangle, |1\rangle\}$ is the *Z-basis*, $\{|+\rangle, |-\rangle\}$ is the *X-basis* and the $\{|+\rangle_y, |-\rangle_y\}$ is the *Y-basis*. Their importance lies in the fact that they are orthonormal basis.

Moreover one can visualize a single qubit by means of the *Bloch Sphere* (Fig. 1.1). Indeed, introducing the real numbers θ, φ, one can write Eq. (1.1) in the following form:

$$|\psi\rangle = \cos\frac{\theta}{2}\,|0\rangle + e^{i\phi}\sin\frac{\theta}{2}\,|1\rangle, \tag{1.4}$$

thus a state is a point on the Bloch Sphere.

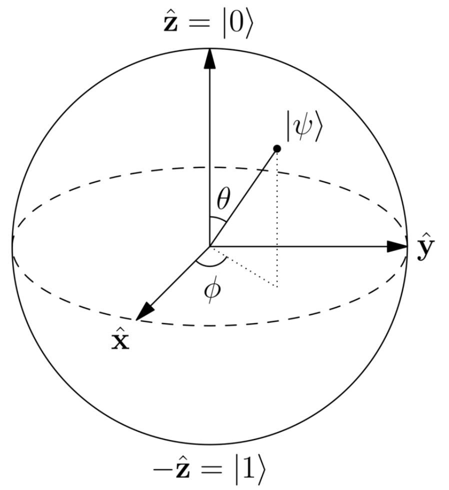

Figure 1.1: *The Bloch Sphere*

Furthermore the basis kets previously introduced correspond to the positive and negative directions of the axis of a Cartesian system:

- $\hat{z} = |0\rangle, -\hat{z} = |1\rangle$,

- $\hat{x} = |+\rangle, -\hat{x} = |-\rangle$,
- $\hat{y} = |+\rangle_y, -\hat{y} = |-\rangle_y$,

which means that measuring the state of a qubit in a given basis corresponds to project the state on one of the three axis depending on which basis is chosen.

1.2 Postulates of Quantum Mechanics

Quantum mechanics can be studied with the formalism of *vector states* [12] or of *density operators* [12], where one is preferred to the other in different situations which will become more clear later. In the following section the postulates for the former will be analyzed, whereas this will be done for the latter in section 1.2.2.

1.2.1 Vector state formalism

As mentioned in the previous section the states live in a Hilbert space. This is stated as the first postulate of quantum mechanics:

Postulate 1.2.1. Associated with any isolated physical system there is a Hilbert space (on $\mathbb{C}$), named *state space* of the system. The system is entirely described by its *state vector* (a unit vector in the state space of the system).

As introduced in Sec. 1.1, the qubits live in a two-dimensional state space. Postulate 1.2.1 requires that the state vector is a unitary vector, i.e. $\langle\psi|\psi\rangle = 1$, which, for a state vector defined as in Eq. 1.1, implies that $|\alpha|^2 + |\beta|^2 = 1$. The condition $\langle\psi|\psi\rangle = 1$ is known asthe *normalization condition*.

In general it is:

$$|\psi\rangle = \sum_i \alpha_i |\phi_i\rangle . \tag{1.5}$$

It is said that the state $|\psi\rangle$ is a *superposition* of the states $|\phi_i\rangle$ with *amplitude* α_i for the state $|\phi_i\rangle$.

A system will eventually undergo an evolution. The description of the evolution of a closed system is given in the following postulate:

Postulate 1.2.2. The evolution of a closed quantum system is described by an *unitary transformation*. That is, given the state $|\psi\rangle$ at time t and the state $|\psi'\rangle$ at time t',

$$|\psi'\rangle = U |\psi\rangle , \tag{1.6}$$

where U is an unitary operator which depends only on t and t'.

One may want a more general formulation of the time evolution of a closed system, as the one given before refers to two precise moments in time. Indeed more in general the evolution of a *closed* quantum system is fully described by the *Schroedinger equation*:

$$i\hbar \frac{d\left|\psi\right\rangle}{dt} = H\left|\psi\right\rangle, \tag{1.7}$$

where H is an Hermitian operator called *Hamiltonian* of the closed system, whose knowledge gives a complete understanding of the system's dynamics. It needs to be said that once the system is coupled with the environment the system becomes *open* and therefore what just stated ceases to be true in the simple way shown in Eq. (1.7).

In Physics measurements are of crucial relevance. The following postulate describes how a measurement can be viewed mathematically and how it affects the state of the given system.

Postulate 1.2.3. Quantum measurement are described by a set $\{M_m\}$ of *measurement operators.* They operate on the state space of the system being measured. If a system is in the state $|\psi\rangle$ before being measured, the probability that the outcome of the measure is m is

$$p(m) = \langle\psi|M_m^\dagger M_m|\psi\rangle \tag{1.8}$$

and the system is left in the state

$$|\psi'\rangle = \frac{M_m\left|\psi\right\rangle}{\sqrt{\langle\psi|M_m^\dagger M_m|\psi\rangle}}. \tag{1.9}$$

Furthermore the $\{M_m\}$ satisfy the *completeness relation*

$$\sum_m M_m^\dagger M_m = I, \tag{1.10}$$

which represents the fact that probabilities sum to one ($\sum_m p(m) = 1$).

When an observable is described by an Hermitian operator M it admits a spectral decomposition

$$M = \sum_m m P_m, \tag{1.11}$$

where P_m is the projector onto the eigenspace of M with eigenvalue m. As $P_m^\dagger = P_m$ and as $P_m^2 = P_m$ (projectors are Hermitian, idempotent and $P_m P_{m'} = \delta_{m,m'} P_m$), from Eq. (1.8) and (1.9) follow:

$$p(m) = \langle\psi|P_m|\psi\rangle \tag{1.12}$$

$$|\psi'\rangle = \frac{P_m\left|\psi\right\rangle}{\sqrt{\langle\psi|P_m|\psi\rangle}}. \tag{1.13}$$

Projective measurements have some handy properties, such as a simple way to compute the mean, which will not be discussed as not relevant for the purposes of this dissertation.

When one is not interested in the state of the system after the measurement has been completed, the *POVM measurements* can be useful. Given Eq. (1.8), is thus defined $E_m = M_m^\dagger M_m$, which simplifies the probability expression to

$$p(m) = \langle\psi|E_m|\psi\rangle \,, \tag{1.14}$$

while the explicit expression (1.9) for the state after the measurement is lost. Furthermore E_m is a positive operator which satisfies the completeness relation $\sum_m E_m = I$. The complete set $\{E_m\}$ is called *POVM* and its elements E_m are known as the *POVM elements* associated with the measurement.

In this dissertation the measurements will be done on qubits, therefore here an example on how to measure the state of a qubit in the computational basis is given.

Example 1.2.1. Given the computational basis $\{|0\rangle, |1\rangle\}$, let

$$\begin{aligned} M_0 &= |0\rangle\langle 0| \\ M_1 &= |1\rangle\langle 1| \,, \end{aligned}$$

which can be easily verified to be the projectors onto the subspaces $|0\rangle$ and $|1\rangle$, respectively. In general a qubit is in the state $|\psi\rangle = \alpha|0\rangle + \beta|1\rangle$. By applying the two operators on the state, one obtains

$$\begin{aligned} p(0) &= \langle\psi|M_0|\psi\rangle = |\alpha|^2 \quad |\psi'\rangle = \frac{M_0|\psi\rangle}{|\alpha|} = |0\rangle \\ p(1) &= \langle\psi|M_1|\psi\rangle = |\beta|^2 \quad |\psi'\rangle = \frac{M_1|\psi\rangle}{|\beta|} = |1\rangle \,, \end{aligned}$$

where in the last step for both a phase has been neglected.

If one wishes to continue the description of the system, the density operator formalism is required, which will be discussed in Sec. 1.2.2.

When dealing with quantum circuits is sure to stumble upon a composite system, namely, in a quantum circuit, multiple qubits. In order to manage them a mathematical tool to describe them is needed and this is accomplished by the following postulate:

Postulate 1.2.4. The state space of a composite physical system is the tensor product of the state spaces of the component physical systems.

Given all what was mentioned in this section one is ready to understand how systems being in a pure state are described. Nevertheless this is not always the case, as for example when environmental decoherence is taken into account, or, as already mentioned, when one makes a measure. Indeed in these cases pure states will be turned into mixtures, for which the density matrix formalism is needed.

1.2.2 Density operator formalism

When a system state is not completely known one turns to the density operator formalism.

Definition 1.2.1. Suppose that a system is in one of the states in the *ensemble of pure states* $\{p_i, |\psi_i\rangle\}$, where each state $|\psi_i\rangle$ has the probability p_i. The *density operator* of the system, also known as *density matrix*, is defined by

$$\rho = \sum_i p_i |\psi_i\rangle \langle\psi_i| . \tag{1.15}$$

It is now possible to clearly explain the difference between a *pure state* and a *mixed state*. A *pure state* of a quantum system is denoted by a vector $|\psi\rangle$ with unit length, i.e. $\langle\psi|\psi\rangle = 1$, in a complex Hilbert space, as defined in postulate 1.2.1. One can construct the operator

$$\rho = |\psi\rangle \langle\psi| , \tag{1.16}$$

which is a projector.

Now one can introduce a mixture of pure states, i.e. the system is in one of the states in the ensemble of pure states $\{p_i, |\psi_i\rangle\}$. Thus ρ, as defined in Eq. (1.15), is in a *mixed state*; it is said to be a *mixture* of the different pure states in the ensemble.

There is a way to distinguish if a system is pure or mixed and it is given by the following theorem:

Theorem 1.2.1. ***Criterion to decide if a state is mixed or pure.*** *ρ is a pure state if and only if $\rho^2 = \rho$.*

Proof. Now ρ is Hermitian, as will be explained by theorem (1.2.2). Therefore it admits a spectral decomposition

$$\rho = \sum_j \lambda_j |j\rangle \langle j| ,$$

where the $\lambda_j \in \mathbb{R}$ are the eigenvalues of ρ and $|j\rangle$ are orthogonal vectors.

For a pure state it is $\rho = |j\rangle \langle j|$, therefore $\rho^2 = \rho$.

In general one has

$$\rho^2 = \sum_{j,k} \lambda_j \lambda_k |j\rangle \langle j|k\rangle \langle k| = \sum_j \lambda_j^2 |j\rangle \langle j| + \sum_{k\neq j} \lambda_j \lambda_k \langle j|k\rangle |j\rangle \langle k| = \sum_j \lambda_j^2 |j\rangle \langle j| .$$

Thus

$$\rho^2 = \rho$$
$$\sum_j \lambda_j^2 |j\rangle \langle j| = \sum_j \lambda_j |j\rangle \langle j| ,$$

which is true if and only if

$$\lambda_j^2 = \lambda_j \Leftrightarrow \lambda_j = 0 \text{ or } \lambda_j = 1.$$

Given the fact that the trace of a density operator is equal to one, as shown in theorem 1.2.2, one has that only one $\lambda_j = 1$ and the others λ_j are zero, which means that the system is in a pure state. □

Before stating new postulates for the density operator it is appropriate to describe it more thoroughly, by giving a mean by which the class of density matrices can be characterized.

Theorem 1.2.2. ***Characterization of density operators.*** *An operator ρ is the density operator associated to an ensemble $\{p_i, |\psi_i\rangle\}$ if and only if ρ is Hermitian, the trace of ρ is equal to one and ρ is a positive operator.*

Proof.

- Given the definition (1.15) of a density operator, one can easily compute

  $$\rho^\dagger = \Big(\sum_i p_i \left|\psi_i\right\rangle \left\langle\psi_i\right|\Big)^\dagger = \sum_i p_i^* (\left|\psi_i\right\rangle \left\langle\psi_i\right|)^\dagger = \sum_i p_i \left|\psi_i\right\rangle \left\langle\psi_i\right| = \rho,$$

  proving indeed that a density operator is Hermitian.

- If ρ is a density operator, then from its definition it follows that

  $$\mathrm{Tr}(\rho) = \mathrm{Tr}\Big(\sum_i p_i \left|\psi_i\right\rangle \left\langle\psi_i\right|\Big) = \sum_i p_i \,\mathrm{Tr}(\left|\psi_i\right\rangle \left\langle\psi_i\right|) = \sum_i p_i = 1$$

  as the $|\psi_i\rangle$ are unit vectors and the sum of probabilities in normalized to one.

- As for the positivity, let $|\phi\rangle$ be any vector in the state space. Thus

  $$\langle\phi|\rho|\phi\rangle = \langle\phi|(\sum_i p_i \left|\psi_i\right\rangle \left\langle\psi_i\right|)|\phi\rangle = \sum_i p_i \left\langle\phi|\psi_i\right\rangle \left\langle\psi_i|\phi\right\rangle = \sum_i p_i| \left\langle\phi|\psi_i\right\rangle|^2 \geq 0$$

  always, as it is product of to surely positive quantities.

- Conversely, if ρ is a Hermitian operator it means that it has a spectral decomposition

  $$\rho = \sum_j \lambda_j \left|j\right\rangle \left\langle j\right|,$$

  where the $\lambda_j \in \mathbb{R}$ are the eigenvalues of ρ and $|j\rangle$ are orthogonal vectors. Thus, given any vector in the state space $|\phi\rangle$,

  $$\langle\phi|\rho|\phi\rangle = \langle\phi|\Big(\sum_j \lambda_j \left|j\right\rangle \left\langle j\right|\Big)|\phi\rangle = \sum_j \lambda_j \left\langle\phi|j\right\rangle \left\langle j|\psi\right\rangle = \sum_j \lambda_j| \left\langle\phi|j\right\rangle|^2 \geq 0,$$

if and only if $\lambda_j \in \mathbb{R}^+$, thus proving that ρ is also positive if this last condition is satisfied, which is the case if λ_j are probabilities. Finally imposing the trace condition $\mathrm{Tr}(\rho) = 1$,

$$\begin{aligned}\mathrm{Tr}\Big(\sum_j \lambda_j \left|j\right\rangle \left\langle j\right|\Big) &= 1\\ \sum_j \lambda_j \,\mathrm{Tr}(\left|j\right\rangle \left\langle j\right|) &= 1\\ \sum_j \lambda_j &= 1.\end{aligned}$$

Thus a system in a state $\left|j\right\rangle$ with probability λ_j will have ρ as the density operator associated with the ensemble $\{\lambda_j, \left|j\right\rangle\}$.

□

A density operator can be thus defined to be a Hermitian and positive operator with trace equal to one.

The postulate 1.2.1 given in the previous section for a pure state can be reformulated for the density operator.

Postulate 1.2.5. Associated with any isolated physical system there is a Hilbert space (on $\mathbb{C}$), named *state space* of the system. The system is completely described by its *density operator* which is a Hermitian and positive operator ρ with trace one, acting on the state space of the system. If a quantum system is in the state ρ_i with a probability p_i then the density operator of the system is $\sum_i p_i \rho_i$.

It is worth noting that while a certain ensemble of quantum states uniquely defines a density matrix, the opposite is not true. Take for instance

$$\left|a\right\rangle = \sqrt{\frac{1}{2}}\left|0\right\rangle + \sqrt{\frac{1}{2}}\left|1\right\rangle \tag{1.17}$$

$$\left|b\right\rangle = \sqrt{\frac{1}{2}}\left|0\right\rangle - \sqrt{\frac{1}{2}}\left|1\right\rangle, \tag{1.18}$$

and the quantum state is prepared in state $\left|a\right\rangle$ with probability 1/2 and in state $\left|b\right\rangle$ with probability 1/2. This ensemble will give the density matrix, by definition (1.15):

$$\rho_{ab} = \frac{1}{2}\left|a\right\rangle\left\langle a\right| + \frac{1}{2}\left|b\right\rangle\left\langle b\right| = \frac{1}{2}\left|0\right\rangle\left\langle 0\right| + \frac{1}{2}\left|1\right\rangle\left\langle 1\right|. \tag{1.19}$$

If one now takes into account the ensemble $\{(1/2, \left|0\right\rangle), (1/2, \left|1\right\rangle)\}$ the related density matrix will be

$$\rho = \frac{1}{2}\left|0\right\rangle\left\langle 0\right| + \frac{1}{2}\left|1\right\rangle\left\langle 1\right|, \tag{1.20}$$

which is equal to the density matrix in Eq. (1.19), thus showing how a density operator does not uniquely define an ensemble of quantum states.

The evolution of a pure state is described by an unitary transformation U ($|\psi'\rangle = U|\psi\rangle$), then

$$\rho' = \sum_i U p_i |\psi_i\rangle \langle\psi_i| U^\dagger = U\rho U^\dagger,$$

which rises the following postulate:

Postulate 1.2.6. The evolution of a closed quantum system is described by an unitary transformation. That is, given U depending only on the times t and t', the states ρ at time t and ρ' at time t' are related by:

$$\rho' = U\rho U^\dagger. \tag{1.21}$$

As for quantum measurement it is required a bit more of work. Firs of all a linear algebra result must be recalled: given the operator A and the unit vector $|\psi\rangle$, it stands [12]:

$$\mathrm{Tr}(A|\psi\rangle\langle\psi|) = \langle\psi|A|\psi\rangle\,. \tag{1.22}$$

Therefore, given the ensemble $\{p_i, |\psi_i\rangle\}$ and the measurement operator M_m, if the initial state is $|\psi_i\rangle$ then the probability of getting the result m is, given Eq. (1.8):

$$p(m|i) = \langle\psi_i|M_m^\dagger M_m|\psi_i\rangle = \mathrm{Tr}(M_m^\dagger M_m |\psi_i\rangle\langle\psi_i|).$$

From probability theory it is known that $p(m) = \sum_i p(m|i)p_i$ and therefor:

$$p(m) = \sum_i p(m|i)p_i = \sum_i p_i \,\mathrm{Tr}(M_m^\dagger M_m |\psi_i\rangle\langle\psi_i|)$$

and for the linearity of the trace

$$p(m) = \mathrm{Tr}(M_m^\dagger M_m \sum_i p_i |\psi_i\rangle\langle\psi_i|);$$

here, given the definition of the density matrix in Eq. (1.15),

$$p(m) = \mathrm{Tr}(M_m^\dagger M_m \rho). \tag{1.23}$$

After the measurement is carried out the density matrix of the quantum system will be different. Indeed, if the initial state is $|\psi_i\rangle$, than the state after obtaining the measurement m is

$$|\psi_i^m\rangle = \frac{M_m|\psi_i\rangle}{\sqrt{\langle\psi_i|M_m^\dagger M_m|\psi_i\rangle}}. \tag{1.24}$$

This leaves an ensemble of states $\{p(i|m), |\psi_i^m\rangle\}$ to which corresponds the density matrix:

$$\rho_m = \sum_i p(i|m) |\psi_i^m\rangle \langle\psi_i^m| = \sum_i p(i|m) \frac{M_m |\psi_i\rangle \langle\psi_i| M_m^\dagger}{\langle\psi_i|M_m^\dagger M_m|\psi_i\rangle}.$$

Given the Bayes theorem

$$p(i|m) = \frac{p(m|i)p_i}{p(m)}, \tag{1.25}$$

$$\begin{aligned} \rho_m = \sum_i \frac{p(m|i)p_i}{p(m)} \frac{M_m |\psi_i\rangle \langle\psi_i| M_m^\dagger}{\langle\psi_i|M_m^\dagger M_m|\psi_i\rangle} = \\ = \sum_i \frac{\langle\psi_i|M_m^\dagger M_m|\psi\rangle\, p_i}{\mathrm{Tr}(M_m^\dagger M_m \rho)} \frac{M_m |\psi_i\rangle \langle\psi_i| M_m^\dagger}{\langle\psi_i|M_m^\dagger M_m|\psi_i\rangle} = \end{aligned}$$

which gives

$$\rho_m = \frac{M_m \rho M_m^\dagger}{\mathrm{Tr}(M_m^\dagger M_m \rho)}. \tag{1.26}$$

The measurement postulate for the density operator formalism can be stated as:

Postulate 1.2.7. The set $\{M_m\}$ of *measurement operators*, acting on the state space of the system being measured, describes quantum measurements and the index m refers to the outcome of the measurement. If immediately before the measurement is carried out the state of the system is ρ, the probability that the measurement m occurs is given by (1.23) and the state of the system after the measurement is (1.26). Furthermore it is satisfied the *completeness equation* (1.10).

One may be interested in studying a composite system and in this case the following postulate is needed:

Postulate 1.2.8. The state space of a composite physical system is the tensor product of the states space of the component physical systems. If the i-th states is described by the density operator ρ_i, with $i = 1, ..., n$, then the combined state is $\rho = \rho_1 \otimes ... \otimes \rho_n$.

It happens frequently to be interested in a subsystem of a composite quantum system. In such cases their description is provided by the *reduced density operator*.

Reduced density operator

Suppose two physical systems A and B are coupled to form the physical system AB, whose state is therefore described by the density matrix ρ_{AB}. This is for example the case of a quantum system which undergoes a coupling with the environment. Then to analyze the result of the coupling on the system the *reduced density operator* is needed:

Definition 1.2.2.

$$\rho_A = \text{Tr}_B(\rho_{AB}), \tag{1.27}$$

where Tr_B is the *partial trace* over system B. Given any two vectors in the state space of A ($|a_1\rangle$, $|a_2\rangle$), and any two vector of system B ($|b_1\rangle$, $|b_2\rangle$), Tr_B is defined by

$$\text{Tr}_B(|a_1\rangle\langle a_2| \otimes |b_1\rangle\langle b_2|) = \text{Tr}(|b_1\rangle\langle b_2|)\,|a_1\rangle\langle a_2|\,. \tag{1.28}$$

The introduction of the reduced density operator is justified by the fact that it reproduces the correct measurements statistics for measurements made on subsystem A.

Now that the formalism used in this dissertation has been introduced it is time to introduce the tools used in QEC.

1.3 Quantum circuits and quantum gates

Quantum information is carried on qubits, therefore a way to act on them and extract the information is needed. Since qubits are quantum entities their manipulation must follow the postulates given in the previous section. Moreover to visualize the operations one does on the qubits *quantum circuits* have been introduced [12].

As stated in postulate 1.2.2, the evolution of a closed quantum system is carried out by unitary operators. Besides the identity operator I, it is convenient to introduce the most used unitary operators in quantum computing, which are the Pauli operators. As they operate on a two-dimensional complex Hilbert space these will be 2×2 matrices:

$$X = \begin{pmatrix} 0 & 1 \\ 1 & 0 \end{pmatrix} \tag{1.29}$$

$$Y = \begin{pmatrix} 0 & -i \\ i & 0 \end{pmatrix} \tag{1.30}$$

$$Z = \begin{pmatrix} 1 & 0 \\ 0 & -1 \end{pmatrix}. \tag{1.31}$$

Another very useful operator for qubit manipulation is the Hadamard operator:

$$H = \frac{1}{\sqrt{2}}\begin{pmatrix} 1 & 1 \\ 1 & -1 \end{pmatrix}. \tag{1.32}$$

The pictorial representation of the operators just introduced in Eq. (1.29), (1.30), (1.31), (1.32) in quantum circuits is the one that can be seen in Fig. 1.2.

As they will be later exploited in some examples, also rotation operators will be here discussed. Before hand a proof the following lemma can be provided:

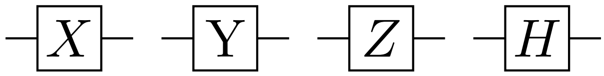

(a) *X gate.* (b) *Y gate.* (c) *Z gate.* (d) *H gate.*

Figure 1.2: *Pictorial representation of the X, Y, Z, H gates.*

Lemma 1.3.1. *Let x be a real number and A a matrix such that $A^2 = I$. Then*

$$\exp(iAx) = \cos(x)I + i\sin(x)A. \tag{1.33}$$

Proof.

$$\exp(ixA) = \sum_{n=0}^{\infty} \frac{(ix)^n A^n}{n!} = \sum_{n_e=0}^{\infty} \frac{(ix)^{n_e} A^{n_e}}{n_e!} + \sum_{n_o=1}^{\infty} \frac{(ix)^{n_o} A^{n_o}}{n_o!}$$

where n_e, n_o denote even and odd indexes respectively. As $A^{n_e} = I$ and $A^{n_o} = A$ the Taylor series for cosine and sine can be spotted and therefore Eq. (1.33) stands. □

Given this results the *rotation operators* about the x, y, z axes are defined by:

$$R_x(\theta) = e^{-i\theta X/2} = \cos\frac{\theta}{2}I - i\sin\frac{\theta}{2}X = \begin{pmatrix} \cos\frac{\theta}{2} & -i\sin\frac{\theta}{2} \\ -i\sin\frac{\theta}{2} & \cos\frac{\theta}{2} \end{pmatrix} \tag{1.34}$$

$$R_y(\theta) = e^{-i\theta Y/2} = \cos\frac{\theta}{2}I - i\sin\frac{\theta}{2}Y = \begin{pmatrix} \cos\frac{\theta}{2} & -\sin\frac{\theta}{2} \\ \sin\frac{\theta}{2} & \cos\frac{\theta}{2} \end{pmatrix} \tag{1.35}$$

$$R_z(\theta) = e^{-i\theta Z/2} = \cos\frac{\theta}{2}I - i\sin\frac{\theta}{2}Z = \begin{pmatrix} e^{-i\theta/2} & 0 \\ 0 & e^{i\theta/2} \end{pmatrix}. \tag{1.36}$$

$$\tag{1.37}$$

Given any direction $\hat{n} = (n_x, n_y, n_z)$, a real unit vector in three dimensions, a generalized rotation by θ around $\hat{n}$ is given by the equation

$$R_{\hat{n}}(\theta) = \exp(-i\frac{\theta}{2}\hat{n}\cdot\vec{\sigma}) = \cos\left(\frac{\theta}{2}\right)I - i\sin\left(\frac{\theta}{2}\right)(n_x X + n_y Y + n_z Z), \tag{1.38}$$

where $\vec{\sigma} = (X, Y, Z)$ is the vector of Pauli matrices.

For the sake of completeness it has to be mentioned that any unitary operator on a single qubit can be written in different ways as a combination of rotations and global phase shifts on the qubit. The following theorem expresses this [12].

Theorem 1.3.2. *Z-Y decomposition for a single qubit.* *Suppose U is a unitary operation on a single qubit. Then there exist real numbers α, β, γ, δ such that*

$$U = e^{i\alpha}R_z(\beta)R_y(\gamma)R_z(\delta). \tag{1.39}$$

This dissertation will discuss more in detail the correction of two specific kind of errors: the *bit-flip* error and the *phase-flip* error. Therefore their definition in terms of the application of an unitary operator is given:

Definition 1.3.1. Bit-flip error. Given a qubit in the state $|\psi\rangle = \alpha|0\rangle + \beta|1\rangle$, a bit flip error is:

$$|\psi\rangle_e = X|\psi\rangle = \alpha|1\rangle + \beta|0\rangle\,, \tag{1.40}$$

which, is easy to verify, is a rotation of π around the x axis up to a global phase.

Definition 1.3.2. Phase-flip error Given a qubit in the state $|\psi\rangle = \alpha|0\rangle + \beta|1\rangle$, a phase flip error is:

$$|\psi\rangle_e = Z|\psi\rangle = \alpha|0\rangle - \beta|1\rangle\,, \tag{1.41}$$

which, is easy to verify, is a rotation of π around the z axis.

However it is important to remark that quantum errors are not discrete, but continuous, as it will be better explained in the next chapter.

When trying to identify whether a *phase-flip* error has occurred it is useful to encode the qubit with an Hadamard gate. Therefore the following identities are of service:

$$HXH = Z, \quad HYH = -Y \quad HZH = X, \tag{1.42}$$

and their proof is a direct computation.

The above mentioned quantum gates are known as *single qubit quantum gates*, but also gates that act on more than one qubit do exist. Indeed when performing quantum error corrections, the *controlled operations* are necessary. The main one, and the one that will be exploited in the following sections, is the *CNOT gate*, which takes as input two qubits, named the *control qubit* and the *target qubit* respectively. Its action is the following: if the control qubit is $|1\rangle$ the target qubit will be flipped, whereas if the control qubit is $|0\rangle$ the target qubit will be left unchanged. Therefore in the computational basis the matrix representation of a CNOT for the $|control, target\rangle$ system is:

$$U_{\text{CNOT}} \equiv CX = \begin{pmatrix} 1 & 0 & 0 & 0 \\ 0 & 1 & 0 & 0 \\ 0 & 0 & 0 & 1 \\ 0 & 0 & 1 & 0 \end{pmatrix}. \tag{1.43}$$

In Fig. 1.3 the circuital representation of a CNOT gate is given: the full dot on the wire is drawn on the control qubit and the circled plus on the wire is drawn on the target qubit.

As it will be useful in the next chapters and to clarify how this gate works, let the control qubit be $|\psi\rangle = \alpha|0\rangle + \beta|1\rangle$ and the target qubit be $|0\rangle$. The state vector of the composite system is $|\Psi\rangle = \alpha|00\rangle + \beta|10\rangle$. Applying the CNOT on this state will leave the system in the state $|\Psi'\rangle = \alpha|00\rangle + \beta|11\rangle$.

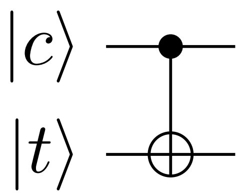

Figure 1.3: *Pictorial representation of a CNOT gate.*

Furthermore the CNOT gate, coupled with the Hadamard gate can create an *entangled* state, which is a composite quantum system which cannot be written as a product of states of its component systems. Indeed with the circuit displayed in Fig. 1.4,

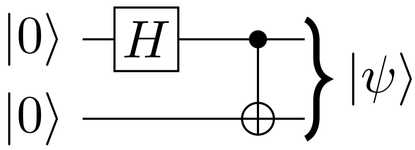

Figure 1.4: *Quantum circuit needed to construct an entangled state.*

the entangled state

$$|\psi\rangle = \frac{|00\rangle + |11\rangle}{\sqrt{2}} \tag{1.44}$$

is built.

Entangled states play a crucial role in quantum information and in quantum computation and for this reason they have been mentioned in this dissertation, but there will not be a deeper analysis as it will lead off-topic.

Another quantum gate which will be mention in Sec. 3.2 is the *SWAP gate*, which swaps the state of the two qubits involved in the operation. Its matrix representation is

$$U_{\text{SWAP}} = \begin{pmatrix} 1 & 0 & 0 & 0 \\ 0 & 0 & 1 & 0 \\ 0 & 1 & 0 & 0 \\ 0 & 0 & 0 & 1 \end{pmatrix}. \tag{1.45}$$

and its pictorial representation is shown in Fig. 1.5.

Only the gates used in this dissertation have been mentioned, but a lot more may be introduced. Furthermore it turns out that universal quantum gates, such as in classical computing, do exist, but this will not be discussed here, as it is not quite relevant for the goal of the dissertation.

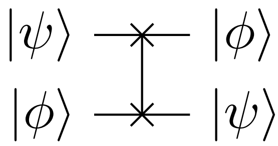

Figure 1.5: *Pictorial representation of a SWAP gate.*

Before passing to the next chapter one last observation is in place: the state vector of a composite quantum system is the tensor product of the state vectors of the systems involved, thus the Hilbert space expands and expanded operators act on it. Indeed suppose one has a composite system composed by n qubits, thus described by the state $|\Psi\rangle = |\psi_1\rangle \otimes \cdots \otimes |\psi_n\rangle$. Then, for instance, if one wants to apply the X Pauli operator on each one of the qubits that compose the system, one has to build the operator $X_n = X \otimes \cdots \otimes X$, where there are n X Pauli operators. In order to lighten the notation it is avoided using the symbol for the tensor product. The following example should clarify the notation: take a system composed by three qubits, then

$$X \otimes I \otimes I \equiv X_1 I_2 I_3, \tag{1.46}$$

meaning that an X operator is acting on the first qubit and identity operators are acting on the second and third qubit.

Chapter 2

Quantum Errors and QEC Codes

While performing quantum computations the qubits are not an isolated system, therefore this interaction leads to noise which can produce errors. QEC deals with how to correct them and thus doing reliable computations. Before diving into more details of quantum errors ad the codes by which they are corrected one has to understand the key aspects of error that occur in quantum computation. Indeed the three following points must be taken into account in order to build QEC algorithms:

- **No cloning**: the no cloning theorem does not allow for a *repetition code* in the classical sense, i.e. copy the bits that carry the information, which is a technique widely used in classical error correction. This means that quantum data cannot be protected by doing multiple copies.

- **Errors are continuous**: a continuum of errors can occur on a single qubit, whereas in classical information the only error is a bit-flip.

- **Measurements destroys quantum information**: measuring a quantum system destroys the quantum state which is being observed, making the recovery impossible.

These facts make classical error correction not suited to quantum information, where different algorithms are needed.

This chapter will discuss the three points just illustrated. Indeed Sec. 2.1 will describe the classical *repetition code* and then give the proof of the *No cloning theorem*. Afterwards Sec. 2.2 will focus on what a quantum error is, disclosing the big differences with the classical error on a bit. Next Sec. 2.3 will talk about *3-qubit codes*. More specifically the processes by which one does the error correction are called *codes* and they work by *encoding* quantum states in a special way that makes them resilient against the effects of noise, and then decoding when it is wished to recover the original state. It is supposed that encoding and decoding can be performed without errors.

More precisely is worth nothing that the error correction protocol will give no information on the coefficients α and β of the vector state of the qubit $|\psi\rangle = \alpha|0\rangle + \beta|1\rangle$. This will be discussed more thoroughly in Sec. 2.3.1. As the key aspect of the *3-qubit codes* is how to extract information without changing the state of the system, Sec. 2.3.2 will explain how this is done in the error correction algorithms for *bit-flip* and *phase-flip* errors. Furthermore to suppress the failure of the code, QEC uses the idea of *redundant encoding*, which means expanding the Hilbert space to a dimension bigger then the one that is needed to store the information given by a single qubit in a way that will be explained in Sec. 2.4. In this section this *encoding* procedure will be thoroughly examined, giving an analytical proof of why this is needed and also a computer simulation to confirm what derived with computations, for an error rate equal on all the qubits of the system. In this section also a computation of the error probabilities if the error rate is different on each qubit is carried out, as it will be needed in Chapter 3.

To conclude, the *9-qubit Shor code* will be presented in Sec. 2.5 in order to give an example of a QEC protocol which can correct for both *bit-flip* and *phase-flip* errors, thus generalizing the ideas used in Sec. 2.3 to do the error detection.

Finally the following remark needs to be addressed: in this chapter it is assumed that all the operations one wish to do on a quantum system are free of errors. For example it is assumed that applying a quantum gate is not affected by errors, which is not the case in the real quantum devices as will become clear in Chapter 3.

2.1 No-cloning theorem

Classical information can be copied. This is exploited when correcting for classical errors. Indeed when one wants to protect a message against an error, the message is *encoded* by adding some redundant information to the message. In this way, if an error takes place, there will be enough information to recover (*decode*) the message and extract the original information. The example of the *binary symmetric channel* should make this clear: suppose a classical bit is sent through a channel which is affected by noise. In the channel the bit will be flipped with probability p whereas with probability $1-p$ there will be no error, with the hypothesis that p is small. To be able to correct an eventual error one can encode $0 \rightarrow 000$ and $1 \rightarrow 111$ (these triplets are called *logical* 0 and 1). Now the three bits are sent through the channel. Suppose the receiver gets 011. Applying the decoding called *majority voting*, since p is small, it is very likely that there has been a *bit-flip* error on the firs bit and the original message was 111. Since the probability of having more than one *bit-flip* error is $3p^2(1-p)+p^3$, the probability of making a mistake using this procedure is $p_e = 3p^2 - 2p^3$. Without the encoding this last probability was p, therefore if $p < 1/2$ it follows that $p_e < p$.

On the other hand quantum mechanics does not allow to copy exactly unknown quantum states, making it impossible to do as just explained for classical information.

This is proved by the **no-cloning theorem** [13], which stands for pure states.

Proof. Suppose there is a copying quantum machine, which can copy an unknown quantum state $|\psi\rangle$ into a target unknown quantum state $|s\rangle$. Therefore the initial state of this machine is

$$|\psi\rangle \otimes |s\rangle .$$

The copying procedure is made by an unitary evolution operator, according to postulate 1.2.2, such that:

$$U(|\psi\rangle \otimes |s\rangle) = |\psi\rangle \otimes |\psi\rangle .$$

If this procedure works for two different pure states, $|\psi\rangle$ and $|\phi\rangle$ it stands

$$\begin{aligned} U(|\psi\rangle \otimes |s\rangle) &= |\psi\rangle \otimes |\psi\rangle \\ U(|\phi\rangle \otimes |s\rangle) &= |\phi\rangle \otimes |\phi\rangle . \end{aligned}$$

To see the nature of the copied quantum systems the inner product of the two hand sides of the last two equations may be taken:

$$\begin{aligned} |\varphi_{1L}\rangle &= U(|\psi\rangle \otimes |s\rangle) \\ |\varphi_{2L}\rangle &= U(|\phi\rangle \otimes |s\rangle) \\ \langle\varphi_{1L}|\varphi_{2L}\rangle &= \langle\psi|\phi\rangle \\ |\varphi_{1R}\rangle &= |\psi\rangle \otimes |\psi\rangle \\ |\varphi_{2R}\rangle &= |\phi\rangle \otimes |\phi\rangle \\ \langle\varphi_{1R}|\varphi_{2R}\rangle &= (\langle\psi|\phi\rangle)^2. \end{aligned}$$

Therefore it stands that

$$\langle\psi|\phi\rangle = (\langle\psi|\phi\rangle)^2.$$

This is formally an equation of the kind $x = x^2$ which has two solutions:

$$\begin{aligned} x = 0 &\Longleftrightarrow \langle\psi|\phi\rangle = 0 \Longrightarrow |\psi\rangle \text{ and } |\phi\rangle \text{ are orthogonal,} \\ x = 1 &\Longleftrightarrow \langle\psi|\phi\rangle = 1 \Longrightarrow |\psi\rangle = |\phi\rangle , \end{aligned}$$

thus implying that a quantum cloning device can only copy states that are orthogonal to one another, making impossible to construct a general quantum cloning device. □

The impossibility to clone quantum states also stands for mixed states, but the details will not be given in this dissertation as it does not concern it directly.

2.2 Quantum errors

As already stated, errors may occur on qubits, namely the state of the quantum systems on which computations are done can change. When it happens it is said that an error occurs. This happens because qubits are not isolated systems and thus they are subjected to noise. One example of this is the coupling of the system under examination with the environment, which leads to *environmental decoherence* [10]. This means that the state of the system is not preserved by time evolution.

To understand this a simple example can be studied: consider a single qubit quantum system and a two level quantum system environment with two basis states $|e_0\rangle$ and $|e_1\rangle$ that satisfy

$$\langle e_i|e_j\rangle = \delta_{ij}, \quad I = |e_0\rangle\langle e_0| + |e_1\rangle\langle e_1|\,. \tag{2.1}$$

When the qubit is in the state $|0\rangle$ nothing happens, while when the qubit is in the state $|1\rangle$ the environmental state is flipped. Finally let the coupling with the environment occur only in the waiting stage of an algorithm; such stage will be mathematically represented by the identity operator I. As the goal is to observe a decoherence between the states $|0\rangle$ and $|1\rangle$, a coherent superposition of these two states is needed to see the effect of the environment. This is achieved by using the Hadamard gate (Eq. (1.32)). Assuming that the environment is initialized in the state $|E\rangle = |e_0\rangle$, it is then coupled with the qubit which is initialized in the state $|\psi\rangle = |0\rangle$:

$$HIH\,|\psi\rangle\,|E\rangle = HIH\,|0\rangle\,|e_0\rangle\,, \tag{2.2}$$

where HIH means that a coherent superposition is applied

$$(HI)\frac{1}{\sqrt{2}}(|0\rangle + |1\rangle)\,|e_0\rangle\,, \tag{2.3}$$

then the coupling with the environment takes place

$$\frac{1}{\sqrt{2}}H(|0\rangle\,|e_0\rangle + |1\rangle\,|e_1\rangle) \tag{2.4}$$

and finally

$$\frac{1}{2}(|0\rangle + |1\rangle)\,|e_0\rangle + \frac{1}{2}(|0\rangle - |1\rangle)\,|e_1\rangle\,. \tag{2.5}$$

Given the definition of the density matrix (Eq. (1.15)), with a direct computation it is found that the density matrix of the state $HIH|0\rangle|e_0\rangle$ is

$$\begin{aligned}\rho =&\frac{1}{4}(|0\rangle\langle 0| + |0\rangle\langle 1| + |1\rangle\langle 0| + |1\rangle\langle 1|)|e_0\rangle\langle e_0| +\\ &\frac{1}{4}(|0\rangle\langle 0| - |0\rangle\langle 1| + |1\rangle\langle 0| - |1\rangle\langle 1|)|e_0\rangle\langle e_1| +\\ &\frac{1}{4}(|0\rangle\langle 0| + |0\rangle\langle 1| - |1\rangle\langle 0| - |1\rangle\langle 1|)|e_1\rangle\langle e_0| +\\ &\frac{1}{4}(|0\rangle\langle 0| - |0\rangle\langle 1| - |1\rangle\langle 0| + |1\rangle\langle 1|)|e_1\rangle\langle e_1| .\end{aligned} \tag{2.6}$$

In order to learn something about our system the use of the reduced density operator is needed as seen in Sec. 1.2.2. Therefore the next step is to trace over the environment part of the total quantum system. This is done using Eq. (1.28) and Eq. (1.22), where in the latter $A = I$ for this example. So, given the orthonormality of the states $|e_0\rangle$, $|e_1\rangle$ (Eq. (2.1)),

$$\begin{aligned}\mathrm{Tr}_E(\rho) =&\frac{1}{4}(|0\rangle\langle 0| + |0\rangle\langle 1| + |1\rangle\langle 0| + |1\rangle\langle 1|)+\\ &\frac{1}{4}(|0\rangle\langle 0| - |0\rangle\langle 1| - |1\rangle\langle 0| + |1\rangle\langle 1|)\\ =&\frac{1}{2}(|0\rangle\langle 0| + |1\rangle\langle 1|),\end{aligned} \tag{2.7}$$

meaning that the coupling with the environment has removed coherences between $|0\rangle$ and $|1\rangle$ states and the second Hadamard transform does not bring back the system in the initial state, which was $|0\rangle$, leaving the system in a *complete mixture* of the two qubit states.

After this first example which gives an idea of how an error may occur when the qubits are coupled with the environment, the focus will be now put on two types of errors for which error correction codes will be introduced in the next sections: *bit-flip errors* and *phase-flip errors*.

Having a *bit-flip error* is equivalent to have an X operator applied on a qubit:

$$|0\rangle \rightarrow |1\rangle \leftrightarrow X|0\rangle = |1\rangle , \tag{2.8}$$

while having a *phase-flip error* is equivalent to have a Z operator applied on a qubit:

$$|+\rangle \rightarrow |-\rangle \leftrightarrow Z|+\rangle = |-\rangle , \tag{2.9}$$

where the computational basis and the X-basis are used in a way that makes the errors more appreciable. In order to correct for these errors it is preferable to *encode* the qubit as explained in Sec. 2.4. This is somehow in analogy to what is done in classical information processing, but the means by which this is done are different. Indeed it has already been explained in Sec. 2.1 how it is not possible to adopt the same procedure used in the *binary symmetric channel* while manipulating quantum information. This matter will be addressed more in detail in the next section.

2.3 3-qubit codes

In order to perform error correction on a qubit one has to find a different procedure from the classical *repetition code*, as proven in Sec. 2.1. A first example of how to achieve QEC are the *3-qubit Shor codes* for *bit-flip* and *phase-flip* errors. It is though important to remark that the 3-qubit code is not a *full quantum code*, as it cannot simultaneously correct for both a bit and a phase-flip error. This will be achieved with the *9-qubit Shor code* which will be discussed in Sec. 2.5.

For *3-qubit Shor codes* [10] the fundamental structure of the algorithm is the same for both the type of errors just mentioned:

1. There is a qubit in the state $|\psi\rangle$ which contains some information that we wish to preserve.

2. In order to better protect against errors this qubit is encoded (in the example of Fig. 2.1 with other two qubits prepared in the state $|0\rangle$) mapping $|\psi\rangle \longrightarrow |\psi\rangle_L$ which is the *logical qubit*.

3. It is assumed that an error may only occur between *encoding* and the error correction process.

4. After the time when an error may occur the error detection takes place. For this process an ancillary system is needed in order to perform *syndrome measurements*, namely extracting information from a system by performing a measurement, but without changing the state of the system. Furthermore the ancilla system is not affected by errors.

5. If an error is detected it is corrected.

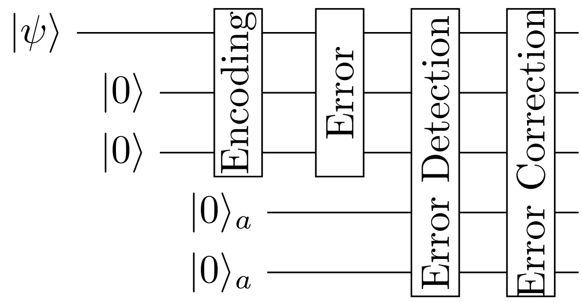

Figure 2.1: *General scheme of how a 3-qubit error correction code works.*

Even though explaining what each step in Fig. 2.1 following a left-to-right order would be preferable, a thorough understanding of the encoding procedure cannot be achieved without first understanding what a *syndrome measurement* is. Therefore now the focus will be put on the latter matter firstly in a more general framework in Sec. 2.3.1, then describing the *3-qubit Shor codes* for *bit-flip* and *phase-flip* errors in Sec. 2.3.2 as a more concrete example of how such a type of measurement can be done on a quantum system and finally analyze thoroughly the encoding procedure in Sec. 2.4, thus understanding why is preferable to encode the initial qubit $|\psi\rangle$.

2.3.1 Syndrome measurement

As stated by postulate 1.2.3, once one performs a measurement on a quantum system, the state of this system changes irreversibly. This is not what one wants while performing *error detection*. Indeed when one performs a measurement which tells what error, if any, has occurred on the state, a result is given which is called *error syndrome*. While doing this no information is given about the coefficients of the linear combination of the basis's vectors in which the state is. The following example should clarify how this works. Let the initial state be $|\psi\rangle = \alpha|0\rangle + \beta|1\rangle$, thus the encoded state is $|\psi\rangle_L = \alpha|000\rangle + \beta|111\rangle$. Now a bit-flip error happens on the first qubit therefore leaving the system in the state $|\psi'\rangle_L = \alpha|100\rangle + \beta|011\rangle$. The error syndromes correspond to the four projection operators [12]:

$$P_0 = |000\rangle\langle 000| + |111\rangle\langle 111|, \quad (2.10)$$
$$P_1 = |100\rangle\langle 100| + |011\rangle\langle 011|, \quad (2.11)$$
$$P_2 = |010\rangle\langle 010| + |101\rangle\langle 101|, \quad (2.12)$$
$$P_3 = |001\rangle\langle 001| + |110\rangle\langle 110|, \quad (2.13)$$

which respectively correspond to no error, bit-flip on qubit one, bit-flip on qubit two, bit-flip on qubit three. If one measures the probabilities $\langle\psi'|P_i|\psi'\rangle_L = \delta_{i,1}$ meaning the *error syndrome* is certainly one for the projector P_1. By eq. (1.13):

$$|\psi''\rangle_L = \frac{P_1|\psi'\rangle_L}{\sqrt{\langle\psi'|P_1|\psi'\rangle_L}} = \alpha|100\rangle + \beta|011\rangle, \quad (2.14)$$

revealing that the quantum state is left unchanged. Anyway in the following in order to extract information regarding possible errors on the data block, i.e. the three encoded qubits, an ancillary system is introduced, making possible to avoid discriminating the exact state of any qubit. To see how the ancillary system works the *3-qubit Shor code* can be taken as reference.

2.3.2 3-qubit error correction codes

As an introduction to quantum error correction codes the *3-qubit code* will here be studied for both *bit-flip* and *phase-flip* errors. It is though important to remark that the *3-qubit* *code* is not a *full quantum code*, as it cannot simultaneously correct for both a bit and a phase-flip error. This will be achieved with the *9-qubit Shor code* which will be discussed in Sec. 2.5.

First of all suppose there is a single qubit in a state $|\psi\rangle = \alpha\,|0\rangle + \beta\,|1\rangle$ which carries some information to preserve. For reasons that will become clear in Sec. 2.4, in order to correct for a single qubit *bit-flip* or *phase-flip* error with the highest probability of measuring the correct result, the qubit needs to be encoded. In the three qubit code a single logical qubit is encoded into three physical qubits. Thus the two logical states $|0\rangle_L$ and $|1\rangle_L$ are defined as

$$|0\rangle_L = |000\rangle\,, \quad |1\rangle_L = |111\rangle\,, \tag{2.15}$$

such that the state previously defined is mapped to

$$\begin{aligned} |\psi\rangle_L &= CX_{13}CX_{12}\,|\psi\rangle \\ &= CX_{13}CX_{12}(\alpha\,|0\rangle + \beta\,|1\rangle)\,|0\rangle\,|0\rangle \\ &= CX_{13}(\alpha\,|00\rangle + \beta\,|11\rangle)\,|0\rangle \\ &= \alpha\,|000\rangle + \beta\,|111\rangle\,, \end{aligned} \tag{2.16}$$

as shown in Fig. 2.2. In the equation the CX_{ij} operators are CNOTs and the subscript i defines the control qubit whereas the subscript j defines the target qubit.

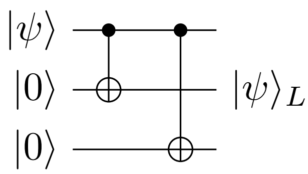

Figure 2.2: *Encoding circuit for a single logical qubit.*

Let $|\psi\rangle_L = |0\rangle_L$. In order to bring the state to $|1\rangle_L$ three bit flips must occur, therefore the *distance* between the two codeword states is $d = 3$. This distance defines the number t of errors that can be corrected [10]:

$$t = \frac{d-1}{2}, \tag{2.17}$$

which in this particular case is $t = 1$, therefore meaning that a three qubit code can only correct one error.

Once the qubit is encoded, two additional ancilla qubits are introduced which will be used to extract *syndrome* information, i.e. information regarding possible errors, from the data block without discriminating the exact state of the three qubits in the data block. For the sake of simplicity it is assumed that the qubits are susceptible to errors only between encoding and correction (Fig. 2.1) and that the gate operations are perfect, even though this is not the case in the real world as will be discussed in Chap. 3.

The next two subsections will examine how to correct for a *bit-flip* or a *phase-flip* separately. A common feature of the two errors is that the detection can be seen from two different point of views: parity between adjacent qubits and the quantum circuit implemented for the error detection. Both are analyzed because the former is conceptually interesting and the latter is crucial to realize working error correction algorithms on real quantum devices.

Bit-flip correction

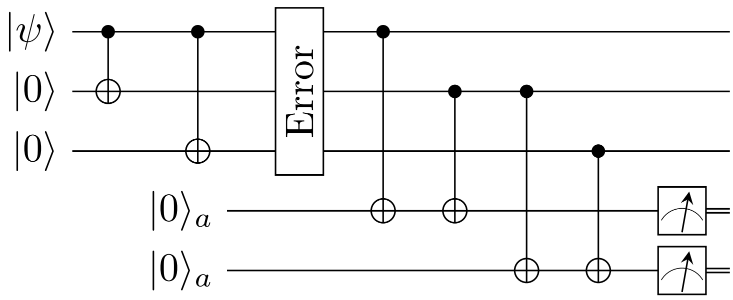

Figure 2.3: *3-qubit error correction circuit for bit-flip errors.*

Now the focus will be driven on a 3-qubit bit-flip error correction code. To achieve this a circuit as the one shown in Fig. 2.3 is needed. At first the single qubit $|\psi\rangle$ is encoded. For the sake of clarity in this section $|\psi\rangle = |0\rangle$ in order to be able to avoid the density matrix formalism, as the action of the CNOTs are thus determined and there is not an ensemble of states (also the state $|1\rangle$ is a good way to go). Then it is assumed that an error may occur and in order to detect it and therefore correct it a two-qubit ancilla system is introduced, denoted by the subscript a. To find out if a bit-flip error has indeed happened the parity between the three qubits must be evaluated, namely, if there is a three qubit system $|q_1q_2q_3\rangle$ and one wants to find out if a bit-flip error has occurred, one measures the parity by applying the Z Pauli operator on two adjacent qubits of the two couples of qubits, for example on q_1q_2, by applying Z_1Z_2, and q_2q_3, by applying Z_2Z_3. This works as the eigenvalues of the Z Pauli operator are $\lambda = \pm 1$:

$$Z|0\rangle = |0\rangle \quad Z|1\rangle = -|1\rangle . \tag{2.18}$$

To better understand what just stated suppose the data block is in a $|000\rangle$ state. Now this state is sent trough a quantum circuit and the receiver wants to find out if a bit-flip error has occurred. This can be achieved using the operator Z to check parity between qubits as it is shown in Tab. 2.1.

received	Z_1Z_2	Z_2Z_3	Error
$\|000\rangle$	$+1$	$+1$	No
$\|100\rangle$	-1	$+1$	X_1
$\|010\rangle$	-1	-1	X_2
$\|001\rangle$	$+1$	-1	X_3

Table 2.1: *Parity using the Z Pauli operator to find out if a bit-flip error has occurred.*

An important remark is in order: if there is more than one bit-flip, the 3-qubit code cannot detect it as all the possible combination of ± 1 are already present in Tab. 2.1.

Going back to the quantum circuit showed in Fig. 2.3, and thus also taking $|\psi\rangle = \alpha|0\rangle + \beta|1\rangle$, the parity is checked via the CNOT gates used after the time when it is supposed an error can occur. The parity is indeed checked by measuring the state of the two ancilla qubits, as shown in Tab. 2.2, where the logical equivalence with Tab. 2.1 is clear.

Ancilla measurement	Collapsed state	Error
00	$\alpha\|000\rangle + \beta\|111\rangle$	No Error
01	$\alpha\|001\rangle + \beta\|110\rangle$	X_3
11	$\alpha\|010\rangle + \beta\|101\rangle$	X_2
10	$\alpha\|100\rangle + \beta\|011\rangle$	X_1

Table 2.2: *Syndrome measurements for the 3-qubit bit-flip code using the quantum circuit in Fig. 2.3.*

As can be seen from Eq. (2.17), the code is not able to correct for more than one error. Indeed if more than one error occurs the code will not detect the right error. This is summarised in Tab. 2.3 and it is in agreement with the result of Eq. (2.17) for the 3-qubit code.

Error occurred	Collapsed state and ancilla	Error detected
$X_1X_2X_3$	$\alpha\|111\rangle\|00\rangle + \beta\|000\rangle\|00\rangle$	No Error
X_1X_2	$\alpha\|110\rangle\|01\rangle + \beta\|001\rangle\|01\rangle$	X_3
X_1X_3	$\alpha\|101\rangle\|11\rangle + \beta\|010\rangle\|11\rangle$	X_2
X_2X_3	$\alpha\|011\rangle\|10\rangle + \beta\|100\rangle\|10\rangle$	X_1

Table 2.3: *The quantum circuit in Fig. 2.3 is not able to detect more than one error.*

Once the syndrome measurement has been performed one is able to correct the error, that has been detected, restoring the initial information, by applying an X gate on the qubit suggested by the detection procedure. It is important to stress again the fact that this is the case only if just an error has occurred, as if more than one qubit has been altered the detection will lead to correct the wrong qubit. For example, taking Tab. 2.3 if an error occurs on both the first and the second qubit the detection procedure will suggest that a bit-flip error has happened on the third qubit, but flipping it back will give a final state which is the flipped of the original one.

Phase-flip Correction

In order to detect a phase-flip error the *encoding* must be done as in Fig. 2.4.

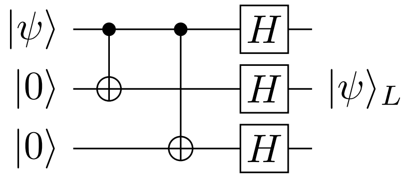

Figure 2.4: *Circuit needed to encode a single qubit for a phase-flip error correction.*

Also in this case syndrome measurement may be performed by doing $H^{\otimes 3}Z_1Z_2I_3H^{\otimes 3} = X_1X_2I_3$ and $H^{\otimes 3}I_1Z_2Z_3H^{\otimes 3} = I_1X_2X_3$, where the use of the Hadamard gates is justified by the identities of Eq. (1.42). As for the case of a bit-flip error, measuring these observables can be viewed as comparing the parity of the pairs of qubits, but this time in the basis introduced in Eq. (1.2). Indeed suppose $|\psi\rangle = 0$, therefore the three qubits will be mapped, by means of the procedure displayed in Fig. 2.4, this way: $|000\rangle \longrightarrow |+++\rangle$. This state is sent to the receiver. In order to determine whether a *phase-flip* error has occurred one measures the observables just cited and obtains the results of Tab. 2.4.

received	X_1X_2	X_2X_3	E
$\|+++\rangle$	$+1$	$+1$	No
$\|-++\rangle$	-1	$+1$	Z_1
$\|+-+\rangle$	-1	-1	Z_2
$\|++-\rangle$	$+1$	-1	Z_3

Table 2.4: *Parity using the X Pauli operator to find out if a phase-flip error has occurred.*

Now the quantum circuits able to measure this parity is shown in Fig. 2.5.

Before analysing how this circuit works one has to understand why it works. A *bit-flip* error changes a state of the computational basis into the other. The same is done by a *phase-flip* error if one operates in the X-basis. Indeed a *phase-flip* error is equivalent to apply the Z Pauli operator, which, when applied on $|+\rangle, |-\rangle$ results in

$$Z|+\rangle = |-\rangle \quad Z|-\rangle = |+\rangle ; \tag{2.19}$$

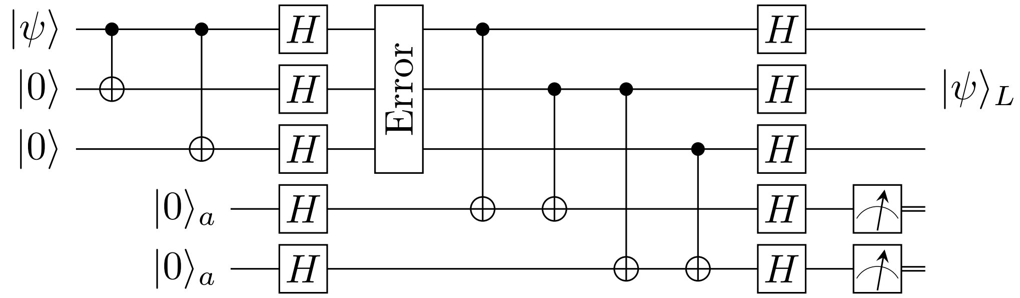

Figure 2.5: *3-qubit error correction circuit for phase-flip errors.*

Also the action of a CNOT is modified:

$$H^{\otimes 2} I_1 X_2 H^{\otimes 2} = I_1 Z_2. \tag{2.20}$$

This means that if also on the ancilla qubits one applies a Hadamard gate before the error detection, the circuit will work formally identically to the one for the bit-flip error. Indeed in order to understand how the code works let $|\psi\rangle = 0$. The encoded logical state will be $|\psi\rangle_L = |+++\rangle$ and at the same time the ancilla state is $|\psi\rangle_a = |++\rangle$. If a phase-flip error occurs on the first qubit then the state will be $|\psi\rangle_L = |-++\rangle$. The CNOT operations for error detection will leave the ancilla state in $|\psi\rangle_a = |-+\rangle$, that will turn into $|\psi\rangle_a = |10\rangle$ after applying again an Hadamard gate on each of the two ancilla qubits. This will suggest that a *phase flip* error has occurred on the first qubit. As for the *bit-flip code*, after detection, correction can be performed.

All the combinations for the syndrome measurement are showed in Tab. 2.5 and, as for the *bit-flip* error correction code, only one *phase-flip* error can be corrected, making of it not a full quantum code.

Ancilla measurement	Collapsed state	Error
00	$\alpha\,|000\rangle + \beta\,|111\rangle$	No Error
01	$\alpha\,|001\rangle + \beta\,|110\rangle$	Z_3
11	$\alpha\,|010\rangle + \beta\,|101\rangle$	Z_2
10	$\alpha\,|100\rangle + \beta\,|011\rangle$	Z_1

Table 2.5: *Syndrome measurements for the 3-qubit phase-flip code using the quantum circuit in Fig. 2.5.*

Moreover by examining the second column of Tab. 2.5, one can see that the collapsed states, which are taken after applying the Hadamard gate following the detection procedure, are the same as the ones for the *bit-flip code*, listed in Tab. 2.2, thus showing once again the formal analogy of the two codes.

Having now understood how the error detection works it is possible to thoroughly focus on the *encoding* procedure. Indeed the encoding is done before the error detection, but to appreciate why it is useful one has to compare the final state, after correction, for an encoded and an unencoded qubit, therefore making necessary to understand the way one can detect errors.

2.4 Why to encode the system

The objective of QEC is to detect and then correct any errors that may occur while processing quantum information. Therefore if one has initially a single qubit in a state $|\psi\rangle = \alpha |0\rangle + \beta |1\rangle$, the aim is to obtain, after the error correction code (Fig. 2.1), a final state $|\phi\rangle = a |0\rangle + b |1\rangle$ as "close" to $|\psi\rangle$ as possible.

The "closeness" of the two states can be evaluated with the concept of *fidelity*:

Definition 2.4.1. Let $|\psi\rangle$ and $|\phi\rangle$ be two vector states. The *fidelity* is

$$F = | \langle\phi|\psi\rangle |^2. \tag{2.21}$$

By this definition a state gets closer to another as F approaches 1, and vice versa, therefore the error correction process needs to leave the system in a state with the highest fidelity possible with the initial state. The *encoding* procedure makes it possible to increase the fidelity between the initial and the final state if the error probability on a single qubit is $p < 0.5$. This can be proven with a simple example which uses as a prototype the *bit-flip* error, but the results are equivalent for the *phase-flip* errror.

2.4.1 Analytical proof

Let $U = \exp(i\epsilon X)$ be coherent errors acting on the qubits, where $\epsilon \ll 1$ (this is a good example of a quantum error as it is a rotation, which is continuous). Coherence is chosen in order to keep the state vector formalism. Now if the unitary operation U is considered acting on a single unencoded logical qubit $|\psi\rangle$, given Eq. (1.33), the state after the error occurs is

$$|\psi\rangle_E = U |\psi\rangle = \cos(\epsilon)I |\psi\rangle + i \sin(\epsilon)X |\psi\rangle \,. \tag{2.22}$$

Therefore the fidelity of the single qubit state is, according to Eq. (2.22),

$$F_{\text{unencoded}} = | \langle\psi|U|\psi\rangle |^2 = \cos^2(\epsilon) \approx 1 - \epsilon^2, , \tag{2.23}$$

as $\epsilon \ll 1$, meaning that the error on the resulting state is of order $O(\epsilon^2)$. Is important to remark that *worst case fidelity* is assumed, namely, in this particular case, $\langle\psi|X|\psi\rangle = 0$, i.e. the state and its bit-flipped are orthogonal. This is however not the general case, but a more thorough explanation of this is provided in Sec. 2.4.3, where understanding this is key to the computer simulation.

Now if the single logical qubit is encoded into three physical qubits as shown in Fig. 2.3 in the part of the circuit before an error may occur, the assumption that each qubit experiences the same error is made and an ancilla system is introduced in order to extract syndrome information. Given the fact that the system is now composed by three qubits, the operators on the system need to be tensorially composed.

Let now the encoded system affected by an error be

$$|\psi\rangle_E = E\,|\psi\rangle_L\,, \tag{2.24}$$

where

$$\begin{aligned} E =& U^{\otimes 3} = (\cos(\epsilon) I + i\sin(\epsilon) X)^{\otimes 3} \\ &= c_0 I_1 I_2 I_3 \\ &+ c_1(X_1 I_2 I_3 + I_1 X_2 I_3 + I_1 I_2 X_3) \\ &+ c_2(X_1 X_2 I_3 + I_1 X_2 X_3 + X_1 I_2 X_3) \\ &+ c_3 X_1 X_2 X_3, \end{aligned} \tag{2.25}$$

and

$$c_0 = \cos^3(\epsilon) \tag{2.26}$$
$$c_1 = i\cos^2(\epsilon)\sin(\epsilon) \tag{2.27}$$
$$c_2 = -\cos(\epsilon)\sin^2(\epsilon) \tag{2.28}$$
$$c_3 = -i\sin^3(\epsilon). \tag{2.29}$$

In order to do a quantitative analysis it is assumed that the error detection works as shown in Fig. 2.3 . Let all the operations carried out in the error detection procedure in Fig. 2.3 be summarized in the operator U_{QEC}, thus:

$$\begin{aligned} U_{QEC}(E\,|\psi\rangle_L\,|00\rangle) =& c_0\,|\psi\rangle_L\,|00\rangle \\ &+ c_1 X_1 I_2 I_3\,|\psi\rangle_L\,|10\rangle \\ &+ c_1 I_1 X_2 I_3\,|\psi\rangle_L\,|11\rangle \\ &+ c_1 I_1 I_2 X_3\,|\psi\rangle_L\,|01\rangle \\ &+ c_2 X_1 X_2 I_3\,|\psi\rangle_L\,|01\rangle \\ &+ c_2 I_1 X_2 X_3\,|\psi\rangle_L\,|10\rangle \\ &+ c_2 X_1 I_2 X_3\,|\psi\rangle_L\,|11\rangle \\ &+ c_3 X_1 X_2 X_3\,|\psi\rangle_L\,|00\rangle\,, \end{aligned} \tag{2.30}$$

where it becomes clear that the QEC algorithm just introduced cannot correct for more than a *bit-flip* error, as the ancillary states if more than one error occurs are the same of the ones that one gets after a single error occurs.

Given what has been detected error correction is made and the collapsed state with correction is in a superposition of $|\psi\rangle_L$ and the logically flipped state $XXX\,|\psi\rangle_L$: $|\phi_{ij}\rangle$, where i, j stands for the state of the ancilla system

$$|\phi_{00}\rangle = c_0\,|\psi\rangle_L + c_3 X_1 X_2 X_3\,|\psi\rangle_L \text{ with the ancilla system in the state } |00\rangle \tag{2.31}$$
$$|\phi_{01}\rangle = c_1\,|\psi\rangle_L + c_2 X_1 X_2 X_3\,|\psi\rangle_L \text{ with the ancilla system in the state } |01\rangle \tag{2.32}$$
$$|\phi_{10}\rangle = c_1\,|\psi\rangle_L + c_2 X_1 X_2 X_3\,|\psi\rangle_L \text{ with the ancilla system in the state } |10\rangle \tag{2.33}$$
$$|\phi_{11}\rangle = c_1\,|\psi\rangle_L + c_2 X_1 X_2 X_3\,|\psi\rangle_L \text{ with the ancilla system in the state } |11\rangle\,. \tag{2.34}$$

If *worst case fidelity* is assumed, $\langle\psi|XXX|\psi\rangle_L = 0$ (prescript L omitted for the sake of legibility), i.e. the two states are orthogonal, the fidelity between the state after no error has been detected with the initial state is, with a suitable normalisation given by the fact that $|c_0|^2 + |c_1|^2 + |c_2|^2 + |c_3|^2$:

$$\begin{aligned} F_{\text{ned}} &= \frac{|\langle\psi|\phi_{00}\rangle|^2}{|\langle\psi|\phi_{00}\rangle|^2 + |\langle\psi|X_1X_2X_3|\phi_{00}\rangle|^2} \\ &= \frac{|c_0\,\langle\psi|\psi\rangle_L|^2}{|c_0\,\langle\psi|\psi\rangle_L|^2 + |c_3\,\langle\psi|\psi\rangle_L|^2} = \frac{|c_0|^2}{|c_0|^2 + |c_3|^2} \\ &= \frac{\cos^6(\epsilon)}{\cos^6(\epsilon) + \sin^6(\epsilon)} \approx 1 - \epsilon^6 \end{aligned} \tag{2.35}$$

which is therefore of order $O(\epsilon^6)$. This state is detected with a certain probability:

$$P_{00} = |00\rangle_{A\,A}\langle 00| \tag{2.36}$$
$$p(|00\rangle_A) = \mathrm{Tr}(P_{00}\,|\phi\rangle\langle\phi|) = \mathrm{Tr}(|00\rangle_{A\,A}\langle 00|\phi\rangle\langle\phi|) = |\langle\phi|00\rangle_A|^2, \tag{2.37}$$

where $|\phi\rangle$ is the state expressed in Eq. (2.30) and the subscript A indicates the ancillary system. Therefore

$$\begin{aligned} p(|00\rangle_A) &= |c_0 + c_3|^2 = |\cos^3(\epsilon) - i\sin^3(\epsilon)|^2 = \cos^6(\epsilon) + \sin^6(\epsilon) \\ &\approx 1 - 3\epsilon^2 + O(\epsilon^4). \end{aligned} \tag{2.38}$$

Thus an error is detected with probability $1 - p(|00\rangle_A) \approx 3\epsilon^2 + O(\epsilon^4)$ and the fidelity between the state in which an error is detected and the initial state, taking any of the $|\phi_{ij}\rangle$ where an error has been detected is given by:

$$\begin{aligned} F_{\text{ed}} &= \frac{|\langle\psi|\phi_{10}\rangle|^2}{|\langle\psi|\phi_{10}\rangle|^2 + |\langle\psi|X_1X_2X_3|\phi_{10}\rangle|^2} \\ &= \frac{|c_1\,\langle\psi|\psi\rangle_L|^2}{|c_1\,\langle\psi|\psi\rangle_L|^2 + |c_2\,\langle\psi|\psi\rangle_L|^2} = \frac{|c_1|^2}{|c_1|^2 + |c_2|^2} \\ &= \frac{\cos^4(\epsilon)\sin^2(\epsilon)}{\cos^4(\epsilon)\sin^2(\epsilon) + \cos^2(\epsilon)\sin^4(\epsilon)} \approx 1 - \epsilon^2. \end{aligned} \tag{2.39}$$

To sum up, if no error is detected the error on the resulting state is suppressed from $O(\epsilon^2)$ to $O(\epsilon^6)$ if the logical qubit is encoded in three physical qubits. If an error is detected the fidelity of the final state is the same, making the encoding procedure useful in order to protect against errors. Indeed as $\epsilon \ll 1$ the majority of correction cycles will detect no error and thus the fidelity of the encoded state will be higher than the unencoded one. Therefore the probability of measuring the correct result at the end of a given algorithm is higher when the system is encoded.

To clarify how the encoding procedure better protects against errors, let the state vector after the error occurs be as the one in Eq. (2.22), where it can be observed that $|i\sin(\epsilon)|^2$ is the probability p that an error has occurred, while $|\cos(\epsilon)|^2$ is the probability $(1-p)$ that no error has occurred. The state can therefore be written as

$$|\psi\rangle_E = \sqrt{1-p}\,|\psi\rangle + \sqrt{p}X\,|\psi\rangle\,. \tag{2.40}$$

By computing the fidelity of this state with the one of the initial qubit, analogously to Eq. (2.23), the fidelity will be

$$F_{\text{ne}}(p) = \cos^2(\epsilon) = 1-p. \tag{2.41}$$

If now one encodes the qubit with other two physical qubits, not considering the terms which account for more than one error, one has:

$$\begin{aligned} E\,|\psi\rangle_L = U^{\otimes 3}\,|\psi_L\rangle &= (\cos(\epsilon)I + i\sin(\epsilon)X)^{\otimes 3}\,|\psi\rangle_L \\ &\approx \cos^3(\epsilon)I_1I_2I_3\,|\psi\rangle_L \\ &+ i\cos^2(\epsilon)\sin(\epsilon)(X_1I_2I_3 + I_1X_2I_3 + I_1I_2X_3)\,|\psi\rangle_L\,, \end{aligned} \tag{2.42}$$

where the computations are analogous to the ones of Eq. (2.30). If, as for the not encoded qubit

$$|\cos^3(\epsilon)|^2 = \cos^6(\epsilon) = (\cos^2(\epsilon))^3 = (1-p)^3 \tag{2.43}$$

$$|i\cos^2(\epsilon)\sin(\epsilon)|^2 = \cos^4(\epsilon)\sin^2(\epsilon) = p(1-p)^2, \tag{2.44}$$

making therefore the final state vector of the system

$$E\,|\psi\rangle_L \approx (1-p)^3\,|\psi\rangle_L + p(1-p)^2(X_1I_2I_3 + I_1X_2I_3 + I_1I_2X_3)\,|\psi\rangle_L\,, \tag{2.45}$$

having therefore a total probability of $3p(1-p)^2$ of having a single error. Once quantum error correction is done the state will be

$$|\psi'\rangle_L \approx [(1-p)^3 + p(1-p)^2]\,|\psi\rangle_L \tag{2.46}$$

and therefore computing the fidelity in the encoded case one finds:

$$F_{\text{e}}(p) = (1-p)^3 + 3p(1-p)^2 \tag{2.47}$$

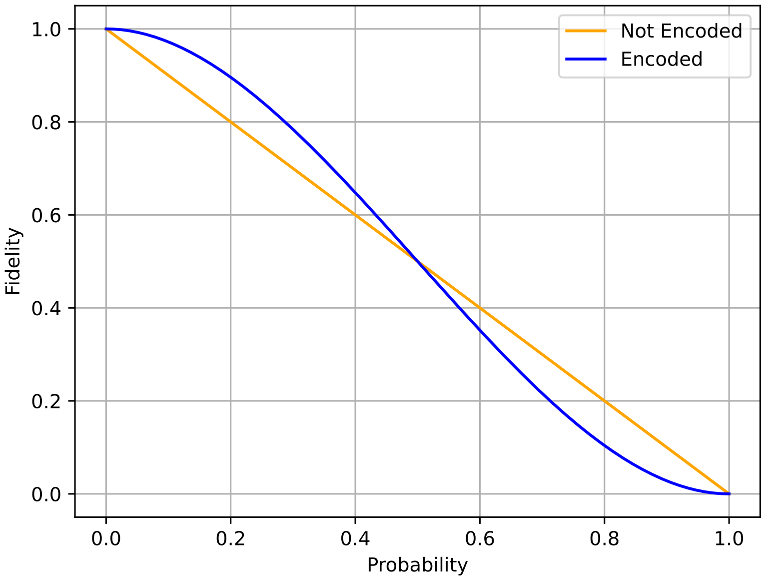

Figure 2.6: *Plot of the fidelities for both an encoded and an unencoded qubit after undergoing a quantum error correction process.*

One can now plot the fidelities for both the cases given by Eq. (2.41) and Eq. (2.47) as shown in Fig. 2.6, where one can see that for little probabilities of an error happening the fidelity of an encoded qubit is higher than the one for an unencoded qubit, making this procedure worth it in the interval of probability $p \in [0, 0.5[$, whereas this situation reverses for $p > 0.5$, where the encoding procedure decreases fidelity respect to the unencoded qubit.

Before going on to the section where results of a computer simulation which verify the computations just done will be displayed, the discussion done for a single error rate ϵ can be extended to a situation in which the error rate on the three qubits is different.

2.4.2 Different error rates on each qubit

What just stated means that the error upon each qubit is represented by

$$E_j = \exp(i\epsilon_j X) \quad j = 1, 2, 3, \tag{2.48}$$

were j labels the qubits. Upon the composite system $|\psi\rangle$ the error operator will be

$$E^{\otimes 3} = E_1 \otimes E_2 \otimes E_3 = \exp(i\epsilon_1 X_1) \exp(i\epsilon_2 X_2) \exp(i\epsilon_3 X_3), \tag{2.49}$$

which can be written as

$$
\begin{aligned}
E^{\otimes 3} &= (\cos(\epsilon_1)I_1 + i\sin(\epsilon_1)X_1)(\cos(\epsilon_2)I_2 + i\sin(\epsilon_2)X_2)(\cos(\epsilon_3)I_3 + i\sin(\epsilon_3)X_3) \\
&= \cos(\epsilon_1)\cos(\epsilon_2)\cos(\epsilon_3)I_1I_2I_3 + i\cos(\epsilon_1)\cos(\epsilon_2)\sin(\epsilon_3)I_1I_2X_3 \\
&+ i\cos(\epsilon_1)\sin(\epsilon_2)\cos(\epsilon_3)I_1X_2I_3 + i\sin(\epsilon_1)\cos(\epsilon_2)\cos(\epsilon_3)X_1I_2I_3 \\
&- \cos(\epsilon_1)\sin(\epsilon_2)\sin(\epsilon_3)I_1X_2X_3 - \sin(\epsilon_1)\cos(\epsilon_2)\sin(\epsilon_3)X_1I_2X_3 \\
&- \sin(\epsilon_1)\sin(\epsilon_2)\cos(\epsilon_3)X_1X_2I_3 - i\sin(\epsilon_1)\sin(\epsilon_2)\sin(\epsilon_3)X_1X_2X_3.
\end{aligned} \tag{2.50}
$$

For a *bit-flip* error the error detection can be done as shown in Fig. 2.3. Denoting with U_{QEC} the operations done to detect the errors, one finds that the final state after detection is:

$$
\begin{aligned}
U_{QEC}E^{\otimes 3}|\psi\rangle_L|00\rangle_A &= \Big(\cos(\epsilon_1)\cos(\epsilon_2)\cos(\epsilon_3) - i\sin(\epsilon_1)\sin(\epsilon_2)\sin(\epsilon_3)\Big)|\psi\rangle_L|00\rangle_A \\
&+ \Big(i\sin(\epsilon_1)\cos(\epsilon_2)\cos(\epsilon_3) - \cos(\epsilon_1)\sin(\epsilon_2)\sin(\epsilon_3)\Big)|\psi\rangle_L|10\rangle_A \\
&+ \Big(i\cos(\epsilon_1)\sin(\epsilon_2)\cos(\epsilon_3) - \sin(\epsilon_1)\cos(\epsilon_2)\sin(\epsilon_3)\Big)|\psi\rangle_L|11\rangle_A \\
&+ \Big(i\cos(\epsilon_1)\cos(\epsilon_2)\sin(\epsilon_3) - \sin(\epsilon_1)\sin(\epsilon_2)\cos(\epsilon_3)\Big)|\psi\rangle_L|01\rangle_A.
\end{aligned} \tag{2.51}
$$

Thus after the error detection has occurred the 5-qubit system can be in one of the 4 states of Eq. (2.31),(2.32),(2.33),(2.34), where this time one has:

$$c_0 = \cos(\epsilon_1)\cos(\epsilon_2)\cos(\epsilon_3) \tag{2.52}$$

$$c_1 = i\Big(\cos(\epsilon_1)\cos(\epsilon_2)\sin(\epsilon_3) + \cos(\epsilon_1)\sin(\epsilon_2)\cos(\epsilon_3) + \sin(\epsilon_1)\cos(\epsilon_2)\cos(\epsilon_3)\Big) \tag{2.53}$$

$$c_2 = -\Big(\cos(\epsilon_1)\sin(\epsilon_2)\sin(\epsilon_3) + \sin(\epsilon_1)\cos(\epsilon_2)\sin(\epsilon_3) + \sin(\epsilon_1)\sin(\epsilon_2)\cos(\epsilon_3)\Big) \tag{2.54}$$

$$c_3 = -i\sin(\epsilon_1)\sin(\epsilon_2)\sin(\epsilon_3). \tag{2.55}$$

Now in order to get the error probability on each qubit one has to compute:

$$|\langle\phi_{00}|(|\psi\rangle_L|00\rangle_A)|^2 \quad \text{no error detected,} \tag{2.56}$$

$$|\langle\phi_{10}|(|\psi\rangle_L|10\rangle_A)|^2 \quad \text{error on qubit 1,} \tag{2.57}$$

$$|\langle\phi_{11}|(|\psi\rangle_L|11\rangle_A)|^2 \quad \text{error on qubit 2,} \tag{2.58}$$

$$|\langle\phi_{01}|(|\psi\rangle_L|01\rangle_A)|^2 \quad \text{error on qubit 3.} \tag{2.59}$$

For instance one can compute the probability of detecting an error on the first qubit by computing Eq. (2.57):

$$\begin{aligned} p(X_1) &= |-i\sin(\epsilon_1)\cos(\epsilon_2)\cos(\epsilon_3) - \cos(\epsilon_1)\sin(\epsilon_2)\sin(\epsilon_3)\,\langle\psi|\psi\rangle_L\,\langle 10|10\rangle_A|^2 \\ &= |-i\sin(\epsilon_1)\cos(\epsilon_2)\cos(\epsilon_3) - \cos(\epsilon_1)\sin(\epsilon_2)\sin(\epsilon_3)|^2 \\ &= \sin^2(\epsilon_1)\cos^2(\epsilon_2)\cos^2(\epsilon_3) + \cos^2(\epsilon_1)\sin^2(\epsilon_2)\sin^2(\epsilon_3) \\ &= \epsilon_1^2(1-\epsilon_2^2)(1-\epsilon_3^2) + (1-\epsilon_1^2)\epsilon_2^2\epsilon_3^2 + O(\epsilon_1^4) + O(\epsilon_2^4) + O(\epsilon_3^4) \\ &\approx \epsilon_1^2, \end{aligned} \tag{2.60}$$

where in the last term all the terms $O(\epsilon_i^4)$ have been omitted. The same can be done to assess the other four probabilities obtaining:

$$p(\text{No error}) = 1 - \epsilon_1^2 - \epsilon_2^2 - \epsilon_3^2 \tag{2.61}$$

$$p(X_1) = \epsilon_1^2 \tag{2.62}$$

$$p(X_2) = \epsilon_2^2 \tag{2.63}$$

$$p(X_3) = \epsilon_3^2. \tag{2.64}$$

These probabilities will be evaluated for real qubits in Chapter 3 using the IBM quantum experience.

2.4.3 Computer simulation proof

Theoretically it turns out that the encoding procedure increases the fidelity between the initial and the final corrected state for an error probability $p \in [0, 0.5[$, whereas for $p \in]0.5, 1]$ the fidelity of the encoded system decreases as compared to the not encoded one. The plots of the theoretical fidelity of an encoded and an unencoded qubit are shown in Fig. 2.6. This can be proven doing a simulation on a classical computer using the Python package *Qutip*, with which one can perform a simulation of the encoding procedure and verify the results just found analytically.

Before diving into the details of the computer simulation it has to be stressed the fact that a classical computer has been used. Indeed this simulation cannot be performed on a quantum computer given the way the measurement is done (more details will be given later).

Hypothesis and initial remarks

The goal is to reproduce numerically the results obtained theoretically in the previous paragraph. In order to do so the same hypothesis done there need to be transported into this analysis. Here it is considered a *bit-flip* error correcting code for an encoded qubit as the one shown in Fig. 2.3. This means that the simulation will be carried out taking as a prototype of error the *bit-flip* error. Furthermore the initial qubit is initialize in the state $|\psi\rangle = |0\rangle$, thus respecting the *worst case fidelity* hypothesis, that is that the bit-flipped state is orthogonal to the original state. The qubits of the logical basis $\{|0\rangle, |1\rangle\}$ respect this and therefore are suitable to be the initial qubits. In the simulations it has been taken that the original qubit is in the state $|0\rangle$. Anyway any other pair of operator and basis that fulfill this requirement could have been taken, for instance the Z Pauli operator, i.e. a phase-flip error, and the X-basis $\{|+\rangle, |-\rangle\}$, which is equivalent to do a simulation for the *phase-flip* error correction code.

Implementation

Established the initial state of the qubit $|\psi\rangle = |0\rangle$ and the error that can occur on the system, *bit-flip* error, one has to distinguish the cases when it is unencoded and when it is encoded. The former is a two-dimensional Hilbert space, therefore operators on this system are 2×2 matrices, while the latter, is the tensor product of three 2-dimensional Hilbert spaces, making it a 8-dimensional Hilbert space. Furthermore when the ancillary system is introduced as be explained in Sec. 2.3 this space gets even large becoming a Hilbert space of dimension 32, thus rising the issue of implementing operators for this space.

For the unencoded qubit the only operator needed is the X Pauli operator (Eq. 1.29), which is already implemented in *Qutip*. Given that also a method for getting the fidelity of two state vectors or two density matrices is offered, there is little work to to for this part of the simulation.

On the other hand for the encoded qubit some operators are needed. The encoding procedure happens in an 8-dimensional Hilbert space and, as seen in Fig. 2.2, CNOT operators acting on this system are needed. In general a *control-operator* gate can be written as

$$CU = |0\rangle\langle 0| \otimes I + |1\rangle\langle 1| \otimes U, \tag{2.65}$$

where $|0\rangle\langle 0|$ is the projector on the subspace of the first qubit, the *control*, and it gives a non-zero term when the control qubit is $|0\rangle$ and the same goes for $|1\rangle\langle 1|$ and $|1\rangle$. From Eq. (2.65) one finds that the *control-not* operator is

$$CX = |0\rangle\langle 0| \otimes I + |1\rangle\langle 1| \otimes X, \tag{2.66}$$

which is easily generalized to more dimensions. In the following the operators without superscripts or subscripts are operators in a two-dimensional Hilbert space and the apex (ij) show on which qubits the operator operates. The CX operator can be generalized for the 8-dimensional Hilbert space as:

$$CX^{(12)} = |0\rangle\langle 0| \otimes I \otimes I + |1\rangle\langle 1| \otimes X \otimes I, \tag{2.67}$$
$$CX^{(13)} = |0\rangle\langle 0| \otimes I \otimes I + |1\rangle\langle 1| \otimes I \otimes X, \tag{2.68}$$

where the former is the CNOT between the first and the second qubit and the latter between the first and the third qubit. Afterwards the ancillary system is introduced, giving a 32-dimensional Hilbert space. Here CNOT gates of greater dimensions are needed, and they are a generalization of Eq. (2.66). Just an example is given as the concept is pretty straight forward:

$$CX^{(14)} = |0\rangle\langle 0| \otimes I \otimes I \otimes I \otimes I + |1\rangle\langle 1| \otimes I \otimes I \otimes X \otimes I. \tag{2.69}$$

Once the system is encoded and the ancillary system is introduced, it is assumed that now and only now an error may occur on any of the three qubits with probability p, thus making necessary the implementation of *bit-flip errors operator* on this system:

$$X^{(1)} = X \otimes I \otimes I \otimes I \otimes I, \tag{2.70}$$

$$X^{(2)} = I \otimes X \otimes I \otimes I \otimes I, \tag{2.71}$$

$$X^{(3)} = I \otimes I \otimes X \otimes I \otimes I. \tag{2.72}$$

It is important to remark that an error may happen independently on any one of the three qubits (not on the ancilla system), thus an error may occur on more than one qubit (indeed this becomes more likely as p increases).

In order to implement the error detection procedure the operators $CX^{(14)}$, $CX^{(24)}$, $CX^{(25)}$, $CX^{(35)}$ are needed. Once the detection procedure is done, as shown in Fig. 2.3 with the operators just defined, the measures are made. To find out the state of the ancillary system the following operators are applied:

$$P^{(00)} = I \otimes I \otimes I \otimes |00\rangle\langle 00|, \tag{2.73}$$

$$P^{(10)} = I \otimes I \otimes I \otimes |10\rangle\langle 10|, \tag{2.74}$$

$$P^{(11)} = I \otimes I \otimes I \otimes |11\rangle\langle 11|, \tag{2.75}$$

$$P^{(01)} = I \otimes I \otimes I \otimes |01\rangle\langle 01|, \tag{2.76}$$

which when applied give $p(m) = 1$ respectively when no error, a bit-flip on the first, second or third qubit is detected. With respect to this measure then the encoded system is corrected, by flippimng back the qubit that the algorithm suggests.

The only thing left to do is to measure the fidelity between the initial state and the final state. As the initial state was $|\psi\rangle = |\psi\rangle_L |00\rangle$ the ancilla system must be in the state $|00\rangle$ after the correction procedure in order to give a non-zero fidelity. Therefore, depending on which error has been detected a bit flip is done on one or more of the ancilla qubits if needed. This measurement procedure is the reason why is not possible to simulate this on a real quantum device: in order to extract information a measurement is done, then using the result of the measurement both the logical qubits and the ancilla qubits are manipulated. This is obviously a procedure that cannot be done on a real quantum system as measurement make the wave function of the system collaps.

Results and conclusions

Once the operators are implemented and the error detection procedure is done one needs to vary the error probability p from zero to one. In each step there is a variation of 0.01. For each one of the 100 probability values the error correction protocol described in the *implementation* paragraph is done and the fidelity is measured 1000 times. Then the mean value of this measurements is plotted as a function of p with an associated error which is the standard deviation of the sample divided by the square root of 1000, i.e. the sample dimension. The result of the simulation is shown in Fig. 2.7 where the theoretical curves are superimposed to the results of the simulation. Without doing a complete data analysis, which is not necessary to the goal of this chapter, one finds that the data harvested from the simulation reproduces what one theoretically aspects, confirming that encoding the qubit which is carrying information is advantageous if $p < 0.5$, which is hopefully the case on real quantum devices.

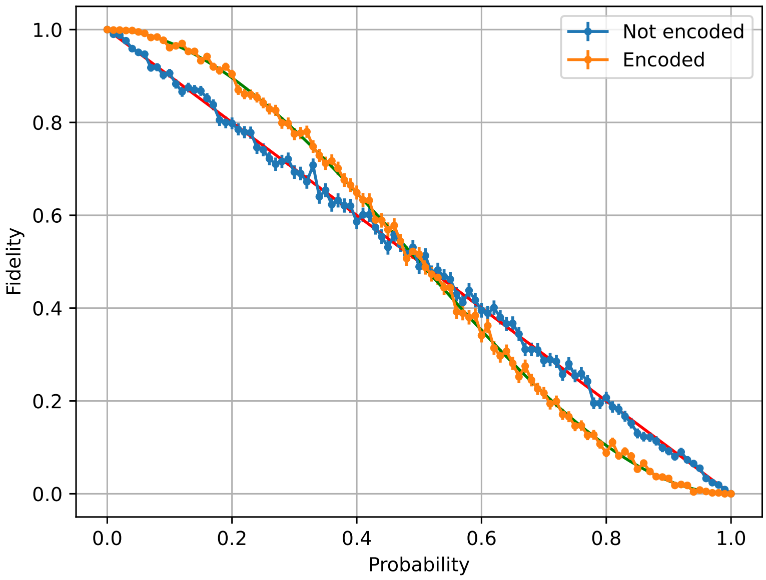

Figure 2.7: *Plot of the fidelities of an encoded and an unencoded qubit given by the simulation procedure described in this section in the worst case fidelity.*

2.5 9-Qubit Code: Shor's Code

The Shor's code [11] is largely based on the 3-qubit code. The circuit needed to encode a single qubit in order to undergo error correction is shown in Fig. 2.8. Therefore the logical encoded state is

$$\begin{aligned}|\psi\rangle_L =& \alpha\,|0\rangle_L + \beta\,|1\rangle_L \\ &= \alpha\frac{1}{\sqrt{8}}(|000\rangle + |111\rangle)(|000\rangle + |111\rangle)(|000\rangle + |111\rangle) \\ &+ \beta\frac{1}{\sqrt{8}}(|000\rangle - |111\rangle)(|000\rangle - |111\rangle)(|000\rangle - |111\rangle).\end{aligned} \tag{2.77}$$

By Eq. (2.17), as $d = 9$, one has $t = 4$. Indeed this code can correct up to a phase-flip error on any of the nine physical quibit and up to a bit-flip error for each group of three qubits. This method of encoding using a hierarchy of levels is known as *concatenation*.

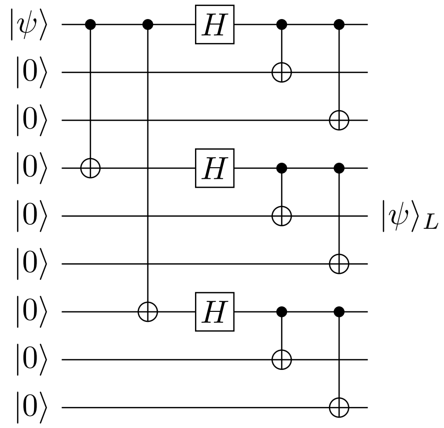

Figure 2.8: *Encoding procedure for the 9-qubit Shor code.*

To understand how this encoding works let $|\psi\rangle = |0\rangle$. The first block of three quibits will be encoded in a state $|\psi'\rangle = (|000\rangle + |111\rangle)/\sqrt{2}$ and, given the CNOTs connecting the first qubit to the fourth and the seventh one, also the other two blocks will be in the state $|\psi'\rangle$, leaving the composed system in the encoded state

$$|\psi\rangle_L = |0\rangle_L = (|000\rangle + |111\rangle)(|000\rangle + |111\rangle)(|000\rangle + |111\rangle)/\sqrt{8}. \tag{2.78}$$

The detection procedure for the bit-flip error on each one of the three blocks of qubits is the same as the 3-qubit code of Sec. 2.3.2, whereas for phase-flip errors they are detected by valuating the parity between two blocks of six qubits as shown in Fig. 2.9, but the concept is the same as for the 3-qubit code. Anyway this time one cannot ensure on which specific qubit the error has occurred, but only on which block.

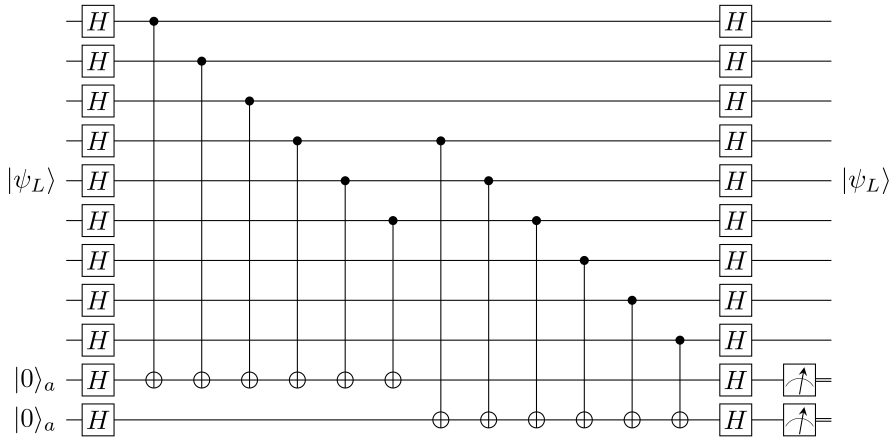

Figure 2.9: *Error detection circuit for the phase-flip error in Shor code.*

Even though, as previously noted, four errors can be detected, the Shor code is a single error correcting code, because it cannot handle multiple errors if they occur in certein locations, for example if two bit-flip errors occur in the same block, as the procedure is the same of the 3-qubit code and it could not manage to detect more than one error.

Chapter 3

Quantum Error Correction with the IBM quantum experience

In Chap. 2 it has been explained what a quantum error is and how to correct it with QEC protocols from a theoretical point of view, namely without dealing with real quantum systems. Indeed also the computer simulation carried out in Sec. 2.4.3 is done using a classical computer not subjected to noise and decoherence as a real quantum device. Given the fact that IBM renders available on the cloud some quantum devices to everyone disposal, it is possible to verify if the algorithms developed in Sec. 2.3.2 actually work in the real world and what are the differences between what theoretically expected and what actually goes on with real qubits, implementing the *3-qubit codes* with the Python module *Qiskit*.

This chapter will therefore describe how what studied in Chap. 2, more specifically the *syndrome measurement*, can be used to evaluate the probability of an error occurring on a qubit (Sec. 3.1). Then in Sec. 3.2 the choice made for the real quantum device to use and its main features will be presented, as they are crucial to understand the results that will be later obtained. The desired algorithms are then implemented on the quantum device using the Python module *Qiskit* in Sec. 3.3. Finally the results will be commented in Sec. 3.4 drawing some conclusions.

3.1 Assessing the error probability on a qubit using the syndrome measurement

As mentioned in the introduction to this chapter, QEC provides algorithms that can correct errors that may occur on qubits while performing some computations. This means that they are algorithms that need to be run in parallel to other ones, in order to make the results of the latter ones reliable. Nevertheless the *syndrome measurement* realized on a quantum circuit presented in Sec. 2.3 has interesting features that can be exploited in order to assess the probability of an error happening on a qubit. In order to do so, one can run the quantum circuit and extract the *error syndrome* many times, then build a histogram of occurrences from which extract the error probability.

To get a better understanding of what just said one can take for instance the quantum error detection protocol pictured in Fig. 2.3 for the *bit-flip* error. Here by measuring the state of the ancilla system after the detection one can get one of the four results $|00\rangle$, $|10\rangle$, $|11\rangle$, $|10\rangle$, meaning that no error, or an error on the first, second or third qubit respectively has been detected. If one measures this state many times and counts the times one obtains a given outcome, the results can be put in a histogram, which will then display the probability of detecting an error on a given qubit. This probability can be simply identified, in a first order approximation as seen in Sec. 2.4.2, with the error probability on a given qubit. The objective of this chapter is indeed to assess this probability for *bit-flip* and *phase-flip* errors using the error detection procedure described in Sec. 2.3.2. Indeed these codes give the possibility to detect if an error has occurred on one of the three qubits of the data block. Therefore the error probability on each one of the three can be evaluated. The other important thing to notice is that the initial qubit, before the encoding procedure takes place, is in a state $|\psi\rangle$, which can be arbitrarily set to any superposition with *Qiskit*. In order to see if there are any differences in the results depending on this initial state, four different ones have been chosen, namely the vectors of the computational basis and the X-basis. This choice has been done as these are the basis in which what *bit-flip* and *phase-flip* errors do is better understandable (as displayed by Eq. (2.8) and Eq. (2.9)). Finally another important difference between the theory and the real devices needs to be pointed out: in the algorithms displayed in Fig. 2.3 and Fig. 2.5 it is assumed that an error may occur only on the data block qubits between the encoding and the error detection procedure, which is not true on real quantum devices.

3.2 Choosing the device

All quantum systems deployed by IBM Quantum are based on superconducting qubit technology [14]. The specifics of this type of hardware are out of the scope of this dissertation. Nevertheless one has to understand a little bit of how they work in order to be able to choose the best device for one's purpose and correctly interpret the results obtained.

First of all one has to deal with the limited number of devices that IBM renders available for free. Indeed if one needs to perform any algorithm involving more than five qubits it is necessary to subscribe for a membership. Luckily five qubits are sufficient to perform the *3-qubit codes*. Now there are four different 5-qubit chips one can choose between. These are all sub-sections of larger devices, which belong to the same architecture (*Falcon*). One of them has undergone its latest revision in January 2021, while the other three got their last revision in April 2020. The one with the latest revision is called *ibmq_manila* and has some better features such a fastest readout, which though does not concern the objective of this dissertation. However there are some differences between the devices just mentioned which do concern it.

The main difference between *ibmq_manila* and the other three is the disposition of the physical qubits, which are shown in Fig. 3.1, where one can see how for *ibmq_manila* (Fig. 3.1a) the qubits are disposed in a linear way, whereas for the other devices (Fig. 3.1b) the qubits are disposed forming a T.

(a) *Physical disposition of the qubits on the device ibmq_manila.*

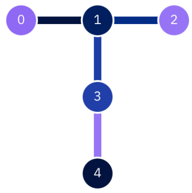

(b) *Physical disposition of the qubits on the other 5-qubit devices.*

Figure 3.1: *Qubit disposition of the 5-qubit quantum devices available.*

At a first glance this could seem harmless, but one has to take into account the fact that CNOT operation can be carried out only between adjacent qubits. Therefore if, for instance, a CNOT has to be performed between qubit 0 and qubit 2 on *ibmq_manila* (Fig. 3.1a), beforehand one of these two qubits has to undergo a SWAP operation (Fig. 1.5) with qubit 1. This brings with it some noise into the final data. Indeed all gates performed on real qubits have an error rate, which has been neglected in Chap. 2 where it has been supposed that the application of a gate can be done perfectly.

Indeed IBM provides tables with the error rates for the main gates one can perform on the qubits such as the X Pauli operator, and the CNOT, whereas no data can be found on the error rate of the SWAP gates. As it concerns the results of the experiment described in Sec. 3.1, the error rates for the CNOT gates have been analyzed. IBM gives information on the error rate between each adjacent qubit of its devices, but in order to make a good choice on which system to use it is sufficient to look at the average error rate of CNOT gates. It turns out that for *ibmq_manila* this is 8.194×10^{-3}, while for the devices with qubits disposed in a T shape the average is 1.747×10^{-2}. Given the fact that the circuit has to be run several times the natural way to go is *ibmq_manila*.

Now the last choice to do is how many times one should run the circuit to get the histogram of occurrences. Given the fact that the CNOT error rate for *ibmq_manila* is approximately of order 10^{-2}, one could think about running the circuit a number of times adequate to have just one hundred CNOTs applied in order to avoid this noise. However, for instance, in the *3-qubit code* for *bit-flip* errors shown in Fig. 2.3 one applies 6 CNOTs for each run (the same goes for the *phase-flip* code), thus, after just approximately 20 runs, this noise will emerge, which is a problem, because 20 measures are certainly not enough to build an histogram of occurrences. Given the fact that evaluating all the noise and finding a proper amount of times to run the circuit will require a deeper understanding of the quantum hardware and a more thorough data analysis, which is not fundamental to this thesis, the number of times that the circuit will be run has been set to 20000, which is the maximum allowed by IBM, having therefore enough entries for the histograms.

3.3 Implementation of the quantum circuits

Once chosen the device and the number of times that the circuits need to be run, the next thing to do is to implement the circuits. As stated in Sec. 3.1 the objective of this chapter is to evaluate the error probability of *bit-flip* and *phase-flip* errors on the qubits using the error detection protocols described in Sec. 2.3.2, employing as initial state the vectors of the computational basis and the X-basis. Thus the implementation of the circuits has to follow these main steps:

- initialization of the five qubits,
- encoding the qubit $|\psi\rangle$ which stores the initial information with other two,
- perform the error detection protocol using the ancilla system,
- measure the state of the ancilla system to extract the *error syndrome*.

Here this processes will be thoroughly analyzed for each one of the four vectors chosen to be the initial states and for the error detection codes for both *bit-flip* and *phase-flip* errors. However in order to avoid useless repetitions the encoding procedure and the detection procedure will be examined just once, for each code, as they obviously work the same for all the initial states $|\psi\rangle$.

First of all one has to initialize the complete circuit of five qubits: a *quantum register* of three qubits which makes up for the data block, a *quantum register* of two qubits which is the ancilla system and two *classical registers* to store the result of the measurement. All this is done with the following commands:

```
from qiskit import *
qr_system = QuantumRegister(3)
qr_ancilla = QuantumRegister(2)
cr_0 = ClassicalRegister(1)
cr_1 = ClassicalRegister(1)
circuit = QuantumCircuit(qr_system, qr_ancilla, cr_0, cr_1)
```

Then one has to initialize the first qubit of *qr_system*, which then needs to be encoded with the other two qubits of *qr_system* before passing through error detection.

3.3.1 Initialization of the first qubit

First of all one must know that by default *Qiskit* initializes all the qubits in the state $|0\rangle$, therefore nothing has to be done when employing this state as the initial state. However when $|1\rangle$ or $|+\rangle$ or $|-\rangle$ are used, the first qubit $|\psi\rangle$ of *qr_system* has to be transformed. As *Qiskit* would have initialized the first qubit in the state $|0\rangle$,

- to obtain the state $|1\rangle$ it is sufficient to apply an X Pauli gate on it (Eq. (1.29)):

$$X|0\rangle = |1\rangle\,, \tag{3.1}$$

  which is done using the command:

```
circuit.x(qr_system[0])
```

- To obtain the state $|+\rangle$ it is sufficient to apply an Hadamard gate H on it (Eq. (1.32)),

$$H|0\rangle = |+\rangle\,, \tag{3.2}$$

  which is done using the command:

```
circuit.h(qr_system[0])
```

- To obtain the state $|-\rangle$ one has to apply an X Pauli gate (Eq. (1.29)) and then a Hadamard gate H (Eq. (1.32)) on it,

$$HX|0\rangle = H|1\rangle = |-\rangle\,, \tag{3.3}$$

  which is done using the commands:

```
circuit.x(qr_system[0])
circuit.h(qr_system[0])
```

All these operations are represented pictorially in Fig. 3.2.

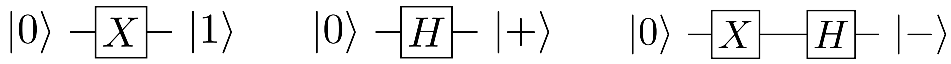

(a) *Operations to obtain* $|\psi\rangle = |1\rangle$.
(b) *Operations to obtain* $|\psi\rangle = |+\rangle$.
(c) *Operations to obtain* $|\psi\rangle = |-\rangle$.

Figure 3.2: *Initialization of the first qubit* $|\psi\rangle$.

The initialization procedure is the same for both the *3-qubit codes* correcting respectively for *bit-flip* and *phase-flip* errors. Anyway the encoding procedure and the error detection procedure are different for the two codes as seen in Sec. 2.3. Therefore the implementation of the two will be carried out separately. For the sake of clarity the discussion in the subsections below will be done employing $|\psi\rangle = |0\rangle$, but the same obviously stands also for the other three initial states.

3.3.2 3-qubit bit-flip error detection code

In order to detect if a *bit-flip* error has occurred the algorithm that needs to be performed is the one displayed in Fig. 2.3. Therefore first of all the encoding procedure needs to be carried out and it can be done using the following commands:

```
circuit.cx(qr_system[0],qr_system[1])
circuit.cx(qr_system[0],qr_system[2])
```

obtaining the circuit shown in Fig. 2.2. After this the detection procedure takes place:

```
circuit.cx(qr_system[0],qr_ancilla[0])
circuit.cx(qr_system[1],qr_ancilla[0])
circuit.cx(qr_system[1],qr_ancilla[1])
circuit.cx(qr_system[2],qr_ancilla[1])
```

and in the end the measurement on the ancilla system can be performed

```
circuit.measure(qr_ancilla[0],cr_0)
circuit.measure(qr_ancilla[1],cr_1)
```

the measurement result thus being stored in the classical register. The complete circuit is shown in Fig. 3.3.

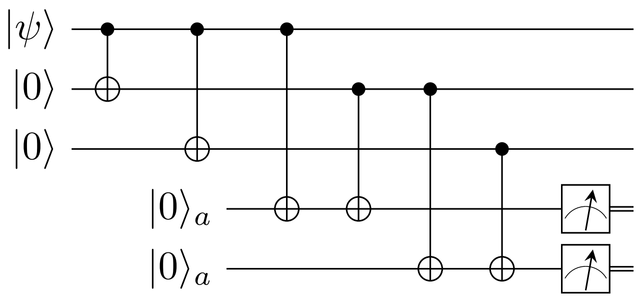

Figure 3.3: *Error detection circuit implemented with Qiskit for the bit-flip error.*

3.3.3 3-qubit phase-flip error detection code

In order to detect if a *phase-flip* error has occurred the algorithm that needs to be performed is the one displayed in Fig. 2.5. Therefore first of all the encoding procedure needs to be carried out and it can be done using the following commands:

```
circuit.cx(qr_system[0],qr_system[1])
circuit.cx(qr_system[0],qr_system[2])
circuit.h(qr_system[0])
circuit.h(qr_system[1])
circuit.h(qr_system[2])
```

obtaining the circuit shown in Fig. 2.4. In this case also the two qubits of the ancillary system need to be modified with an Hadamard gate, thus

```
circuit.h(qr_ancilla[0])
circuit.h(qr_ancilla[1])
```

After this the detection procedure takes place:

```
circuit.cx(qr_system[0],qr_ancilla[0])
circuit.cx(qr_system[1],qr_ancilla[0])
circuit.cx(qr_system[1],qr_ancilla[1])
circuit.cx(qr_system[2],qr_ancilla[1])
```

then an Hadamard gate is applied on each qubit of the system:

```
circuit.h(qr_system[0])
circuit.h(qr_system[1])
circuit.h(qr_system[2])
circuit.h(qr_ancilla[0])
circuit.h(qr_ancilla[1])
```

and in the end the measurement on the ancilla system can be performed

```
circuit.measure(qr_ancilla[0],cr_0)
circuit.measure(qr_ancilla[1],cr_1)
```

the measurement result thus being stored in the classical register. The complete circuit is shown in Fig. 3.4.

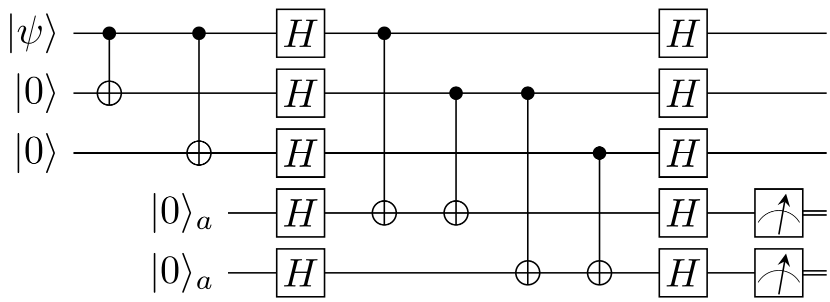

Figure 3.4: *Error detection circuit implemented with Qiskit for the phase-flip error.*

3.4 Results and conclusions

At this point everything is ready to perform the experiments. Therefore the *3-qubit codes* for *bit-flip* and *phase-flip* errors have been run with all the four initial states illustrated in Sec. 3.3.1. More specifically, for each initial state the code has been run for 20000 times as mentioned in Sec. 3.2 and the times in which the ancill state has been measured in one of the four outcomes $|00\rangle$, $|10\rangle$, $|01\rangle$, $|11\rangle$ have been counted. The resulting histograms are illustrated in Fig. 3.5 and in Fig. 3.6 for *bit-flip* and *phase-flip* errors respectively, where on the x axis there is the measured ancilla state and on the y axis the probability of measuring that state.

Now in order to evaluate the error probability, separately for *bit-flip* and *phase-flip* errors, let $p_\alpha^{(i)}$ represent the error probability on the i-th qubit for the initial state $|\psi\rangle = |\alpha\rangle$. To have a more significant value, the error probability will be assessed as a mean of the four values obtained directly by the experiment:

$$\bar{p}^{(i)} = \frac{p_0^{(i)} + p_1^{(i)} + p_+^{(i)} + p_-^{(i)}}{4}. \tag{3.4}$$

To this mean value an error has to be associated:

$$\sigma_{\bar{p}^{(i)}} = \sqrt{\frac{1}{4}\left[(p_0^{(i)} - \bar{p}^{(i)})^2 + (p_1^{(i)} - \bar{p}^{(i)})^2 + (p_+^{(i)} - \bar{p}^{(i)})^2 + (p_-^{(i)} - \bar{p}^{(i)})^2\right]}. \tag{3.5}$$

All the $\bar{p}^{(i)}$ and $\sigma_{\bar{p}^{(i)}}$ are reported in Tab. 3.1 and Tab. 3.2. These values could be more precise carrying out a more thorough data analysis, but this is not the subject of this dissertation.

First of all a comment on the convention that has been followed in the association of the error needs to be done: the error has been taken with two significant digits. Now the results for the two types of error will be displayed and conclusions drowned.

Bit-flip Error

The histograms of occurrences are displayed in Fig. 3.5 and the probabilities with the associated error are shown in Tab. 3.1.

Guessed error	Ancilla state	$\bar{p}$	$\sigma_{\bar{p}}$
No error	00	0.801	0.015
X_1	10	0.0575	0.0047
X_2	11	0.0480	0.0086
X_3	01	0.0935	0.0075

Table 3.1: *Values of the mean probability and its relative errors for the bit-flip error detection code.*

The first thing that can be noticed is that in all cases the probability that no error occurs is the highest. Looking at the probability that an error actually occurs one in principle expects that it should be the same on each one of the three qubits, as there is no reason to establish a priori that a qubit may be more affected by errors than the others. This though is not the conclusion that can be drowned looking at the results in Tab. 3.1, where indeed the probability of a *bit-flip* error happening on the third qubit is

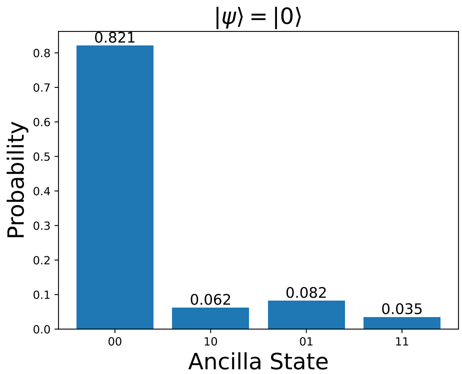

(a) *Histogram of probabilities for* $|\psi\rangle = |0\rangle$.

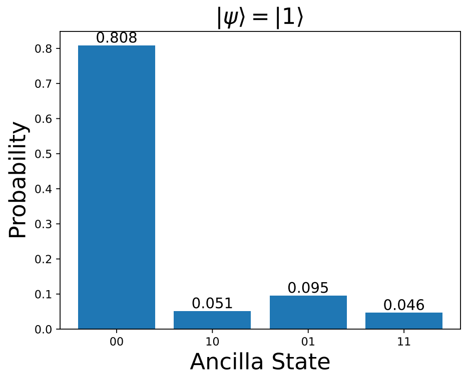

(b) *Histogram of probabilities for* $|\psi\rangle = |1\rangle$.

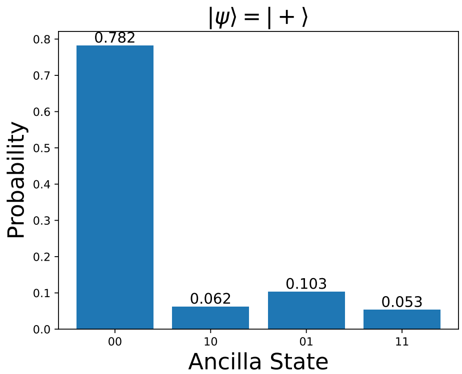

(c) *Histogram of probabilities for* $|\psi\rangle = |+\rangle$.

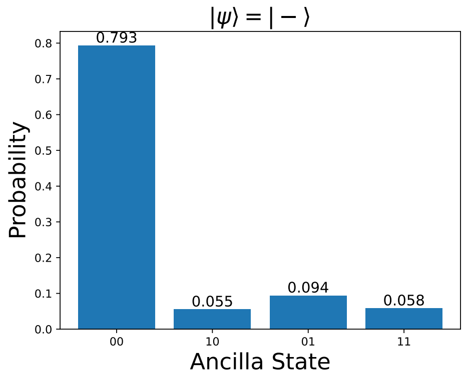

(d) *Histogram of probabilities for* $|\psi\rangle = |-\rangle$.

Figure 3.5: *Histograms for the bit-flip error detection.*

higher then the other two probabilities, which are comparable in the error range. This may depend on many factors and it is difficult to assess the specific reasons why this happen giving the fact that how *Qiskit* swaps the qubits in order to perform CNOTs is unknown, nevertheless some reasons will be pointed out later, since they are valid also for the *phase-flip* error.

Phase-flip error

The histograms of occurrences are displayed in Fig. 3.6 and the probabilities with the associated error are shown in Tab. 3.2.

The first thing that one notices is that the probability of having no errors is the highest. Furthermore one notices by looking at Fig. 3.6 and Tab. 3.2 that even if a priori one expects to have the same phase-flip error probability on each qubit it turns

Guessed error	Ancilla state	$\bar{p}$	$\sigma_{\bar{p}}$
No error	00	0.863	0.025
Z_1	10	0.101	0.025
Z_2	11	0.0058	0.0015
Z_3	01	0.0298	0.0015

Table 3.2: *Values of the mean probability and its relative errors for the phase-flip error detection code.*

out that the first qubit is much more affected by this type of error than the other two, whereas the second qubit is very less likely to be phase-flipped. As for the bit-flip error it is difficult to understand why this happens, but some considerations will be done in the next paragraph.

Comparisons and conclusions

The significant downside to this analysis is the impossibility to be certain of what is the reason why the error rates on the different qubits is not the same, given the fact that in order to perform the algorithm *Qiskit* modifies the order of the qubits on the linear device *ibmq_manila*, thus rendering necessary a very thorough knowledge of the underling quantum hardware and a more thorough data analysis, such as *randomized benchmarking* [15], which both are out of the objective of this theses. Nevertheless some considerations can be done. Indeed the first thing that needs to be pointed out is that the two codes are only able to detect one error, but more than one error may occur, as shown in Tab. 2.3 (it is equivalent also for a *phase-flip* error), leading to another type of noise in the collected data. Indeed even if having more than one error is less probable, in 20000 runs this event surely takes place. Furthermore, as mentioned in Sec. 3.2, the order of the physical qubits is important, since CNOTs can be carried out only on adjacent qubits. Indeed *Qiskit* provides a way to implement a circuit, but then, in the background, it manipulates the qubit on the device in a way suited to carry out the required computations. Therefore all the swaps that go on while running the circuit are unknown and this leads to more noise as well.

However it can be pointed out that, for both the kinds of errors, one qubit is more affected by errors than the others, regardless the initial state of the first qubit $|\psi\rangle$. Indeed for the *bit-flip* error the qubit more affected by it is the third qubit, whereas for the *phase-flip* error it is the first qubit. Once again the reason why this happens cannot be evaluated.

Moreover, as these probabilities include also the effects of noise due to the application of gates and also the errors that may occur on the ancillary system, which have not been taken into account, it can be concluded that these error probabilities are for sure overestimated.

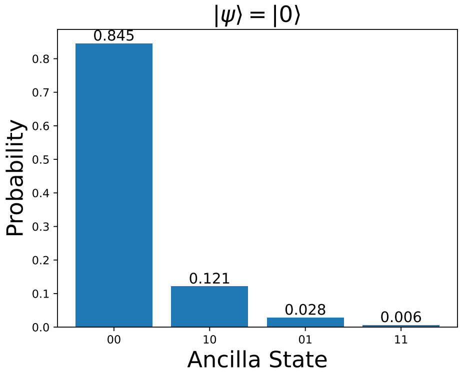

(a) *Histogram of probabilities for* $|\psi\rangle = |0\rangle$.

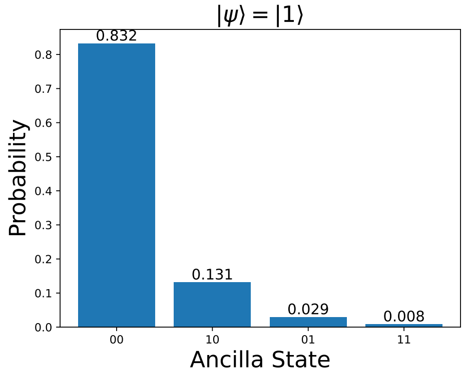

(b) *Histogram of probabilities for* $|\psi\rangle = |1\rangle$.

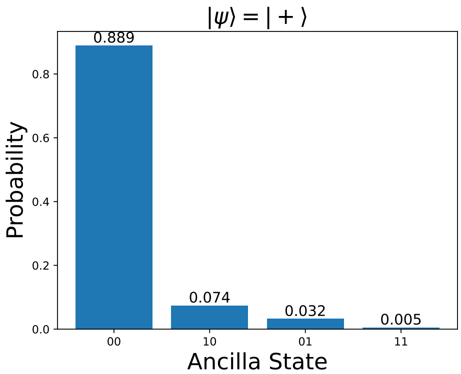

(c) *Histogram of probabilities for* $|\psi\rangle = |+\rangle$.

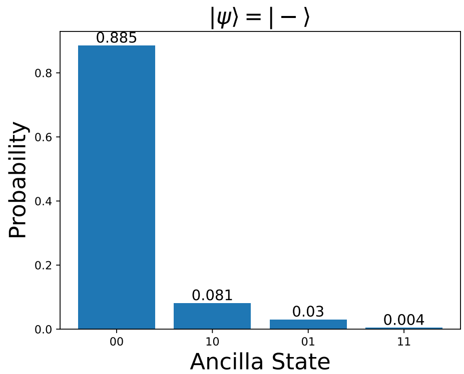

(d) *Histogram of probabilities for* $|\psi\rangle = |-\rangle$.

Figure 3.6: *Histograms for the phase-flip error detection.*

Finally it can be stated that it is more likely to have a *bit-flip* error than a *phase-flip* error, given the fact that the probability of having no error is $\bar{p} = 0.801 \pm 0.015$, for the former, and $\bar{p} = 0.863 \pm 0.025$ for the latter, which are also both significantly higher than having an error on any of the three qubits, thus meaning that most of the time the computation will be correct. Furthermore given the fact that all the error probabilities evaluated in this section are smaller than 0.5 it can be said that the encoding procedure is convenient as proven in Sec. 2.4.

Conclusions

In this thesis, after an introduction on the postulates of Quantum Mechanics (for both pure and mixed states), followed by the study of quantum gates and quantum circuits, Quantum Error Correction has been discussed. This has been done by analyzing the differences with the classical error correction. Firstly the *no-cloning theorem* has been proven, which leads to the necessity of finding another option to protect information from the classical *repetition code*, which is the *encoding* procedure. Then the fact that quantum errors are continuous, differently from the classical ones, has been discussed, pointing out, with an example, how on qubits the errors happen when they are coupled with the environment. Lastly the problem of measurement has been tackled and a solution that allows to extract information from the system, without modifying it, has been found: the *syndrome measurement*, done with an ancilla system. Once described the general framework of QEC, some examples of quantum error correction codes have been presented, namely the *3-qubit codes* for *bit-flip* and *phase-flip* errors and the *9-qubit Shor code*. Then, given its importance in the understanding of how the information carried by qubits can be protected against errors, a detailed study of the *encoding* procedure has been carried out.

In the last chapter the probability of a *bit-flip* and a *phase-flip* error happening on a qubit has been assessed by performing the *syndrome measurements* on the *3-qubit codes*. More precisely a 5-qubit quantum computer, *imbq_manila*, has been employed to run the *3-qubit codes* and, by measuring the state of the ancilla system after the error detection protocol for 20000 times, histograms of occurrences were built from which the error probabilities on each one of the three qubits of the data block could be evaluated. The results showed that the probability of not having a *bit-flip* error is $\bar{p} = 0.801 \pm 0.015$, whereas the probability of not having a *phase-flip* error is $\bar{p} = 0.863 \pm 0.025$. Thus the error probability is not negligible, however the error probability is less than 0.5, hence legitimizing the *encoding* procedure and showing how the QEC theory is indeed applicable on real quantum computers.

Bibliography

[1] F. Arute et al., Quantum Supremacy using a Programmable Superconducting Processor, *Nature* **574** 505 (2019).

[2] M. Saffman, Quantum computing with neutral atoms, *National science review* **6** 24 (2019).

[3] H. Häffner, C. Roos, and R. Blatt, Quantum computing with trapped ions, *Physics Reports* **469** 155 (2008).

[4] H.-L. Huang, D. Wu, D. Fan, and X. Zhu, Superconducting quantum computing: a review, *Science China. Information sciences* **63** (2020).

[5] J. L. O'Brien, Optical Quantum Computing, *Science* **318** 1567 (2007).

[6] V. Lahtinen and J. K. Pachos, A Short Introduction to Topological Quantum Computation, *SciPost Phys.* **3** 021 (2017).

[7] D. Gottesman, Theory of fault-tolerant quantum computation, *Physical Review A* **57** 127 (1998).

[8] S. Krinner et al., Realizing repeated quantum error correction in a distance-three surface code, *Nature* **605** 669 (2022).

[9] L. Postler et al., Demonstration of fault-tolerant universal quantum gate operations, *Nature* **605** 675 (2022).

[10] S. J. Devitt, W. J. Munro, and K. Nemoto, Quantum error correction for beginners, *Reports on Progress in Physics* **76** 076001 (2013).

[11] P. W. Shor, Scheme for reducing decoherence in quantum computer memory, *Phys. Rev. A* **52** R2493 (1995).

[12] M. A. Nielsen and I. L. Chuang. Quantum Computation and Quantum Information. (Cambridge University Press, 2000).

[13] W. K. Wootters and W. H. Zurek, A single quantum cannot be cloned, *Nature* **299** 802 (1982).

[14] M. Steffen, D. P. DiVincenzo, J. M. Chow, T. N. Theis, and M. B. Ketchen, Quantum computing: An IBM perspective, *IBM Journal of Research and Development* **55** 13:1 (2011).

[15] *Randomized Benchmarking*, https://qiskit.org/textbook/ch-quantum-hardware/randomized-benchmarking.html.